Theoretical Notes
Note 272

TN 272

CABLE RESPONSE SOLUTION TECHNIQUES FOR THE SYSTEM-GENERATED ELECTROMAGNETIC PULSE ENVIRONMENT

Volume 1

Methodology and Development of a System Generated Electromagnetic Pulse Cable Code

Eric P. Wenaas
Ronald E. Leadon

Intelcom Rad Tech
P. O. Box 80817
San Diego, CA 92138

May 1976

Final Report

AIR FORCE WEAPONS LABORATORY
Air Force Systems Command
Kirtland Air Force Base, NM 87117

UNCLASSIFIED

SECURITY CLASSIFICATION OF THIS PAGE *(When Data Entered)*

REPORT DOCUMENTATION PAGE		READ INSTRUCTIONS BEFORE COMPLETING FORM
1. REPORT NUMBER AFWL-TR-75-174, Vol. 1	2. GOVT ACCESSION NO.	3. RECIPIENT'S CATALOG NUMBER
4. TITLE *(and Subtitle)* CABLE RESPONSE SOLUTION TECHNIQUES FOR THE SYSTEM-GENERATED ELECTROMAGNETIC PULSE ENVIRONMENT; Vol. 1--Methodology and Development of a System Generated Electromagnetic Pulse Cable Code		5. TYPE OF REPORT & PERIOD COVERED Final Report 6. PERFORMING ORG. REPORT NUMBER INTEL-RT 8111-078
7. AUTHOR(s) Eric P. Wenaas Roland E. Leadon		8. CONTRACT OR GRANT NUMBER(s) F29601-74-C-0039
9. PERFORMING ORGANIZATION NAME AND ADDRESS Intelcom Rad Tech P.O. Box 80817 San Diego, California 92138		10. PROGRAM ELEMENT, PROJECT, TASK AREA & WORK UNIT NUMBERS 64711F 49950310
11. CONTROLLING OFFICE NAME AND ADDRESS Air Force Weapons Laboratory (ELC) Kirtland Air Force Base, NM 87117		12. REPORT DATE May 1976 13. NUMBER OF PAGES 88
14. MONITORING AGENCY NAME & ADDRESS*(if different from Controlling Office)*		15. SECURITY CLASS. *(of this report)* UNCLASSIFIED 15a. DECLASSIFICATION/DOWNGRADING SCHEDULE

16. DISTRIBUTION STATEMENT *(of this Report)*
Approved for public release; distribution unlimited.

17. DISTRIBUTION STATEMENT *(of the abstract entered in Block 20, if different from Report)*

18. SUPPLEMENTARY NOTES
This report consists of two volumes: Vol. 1, Methodology and Development of A SGEMP Cable Code, is by Intelcom Rad Tech; and Vol. 2, Preliminary Estimate of Photon Excitation of Multiconductor Cables, presents supporting analysis by Mission Research Corporation

19. KEY WORDS *(Continue on reverse side if necessary and identify by block number)*
System Generated EMP (SGEMP)
Computer Programs
Radiation Effects
Cable Currents
Satellite Systems Analysis

20. ABSTRACT *(Continue on reverse side if necessary and identify by block number)*
Solution techniques for the System Generated Electromagnetic Pulse (SGEMP) excitation of single- and multiple-wire cables are explored, and a formalism for solving the cable problem is defined. Progress on the development of a computer code for predicting these currents is reported.

DD FORM 1 JAN 73 1473 EDITION OF 1 NOV 65 IS OBSOLETE

UNCLASSIFIED

SECURITY CLASSIFICATION OF THIS PAGE *(When Data Entered)*

CONTENTS

FIGURES

1. INTRODUCTION

1.1 BACKGROUND

The major thrust of the system-generated electromagnetic pulse (SGEMP) code development work to date has been in the structural response area. Computational techniques have been developed to treat the self-consistent space-charge-limited response for two-dimensional bodies of revolutions (Refs. 1,2), and work is on-going to develop useful three-dimensional treatments (Ref. 3).

An equally important area of investigation for system assessment is that of coupling the SGEMP environment to cables. While a significant amount of work has been expended on the direct excitation of shielded cables by x-ray and gamma irradiation (Refs. 4-8), there does not seem to be any thorough treatment of the electromagnetic and direct photon excitation produced by the low-energy photon environment. Thus, the thrust of this effort is directed at developing a formalism for treating the problem and beginning the development of analysis tools deemed appropriate to quantitatively describe the cable response to the SGEMP environment.

Ideally, the ultimate goal of such an effort should be to develop the techniques and capabilities to predict the individual wire currents leading to the circuits. It should be emphasized at the outset, however, that an accurate prediction of the individual response of a single wire in a complex cable harness without significant inputs of experimental data is quite unlikely. Therefore, we do not wish to hold out a false promise that the results of this effort will lead to accurate predictions of wire currents. Rather, we believe that the purpose of a cable response investigation program should be to understand the mechanisms involved; to determine how the response changes with incident fluence, energy, time histories, number and size of cables, etc.; and to provide bounds on individual wire currents.

1.2 APPROACH

The problem is addressed by stating the requirements for a formal, rigorous solution. It is immediately evident that approximations are required to make the problem tractable. Various approximate techniques are introduced, including three- and two-dimensional treatments, each succeeding approximation having less complexity and correspondingly less rigor than the previous one. Wherever possible, liberal use is made of techniques and computer codes developed for ordinary EMP excitation of cables. Modifications and additions to these techniques are indicated where appropriate.

We have chosen to define more than one approximate technique for a given cable configuration, because the suitability or tractability of a given model depends upon the application. In general, the level of detail that can be considered for a single cable bundle in a controlled phenomenology study is far greater than can be considered for system assessment. Thus, a particular approximate technique that may be tractable and reasonably rigorous for an isolated, well defined cable may not be desirable because the time required to obtain the solution. In addition, the cable parameters required in the more rigorous solution may not be obtainable with sufficient accuracy to warrant the detailed solution technique.

Two approaches have been used in this effort in an attempt to define tractable models for both phenomenology studies and systems applications. First, reasonably detailed models are formed with two or three wire bundles to identify important excitation modes and source terms. The idea here is to build a suitably complex tool for phenomenology applications and exercise the tool to determine what simplifications are possible and under what conditions. The disadvantage with this approach is that considerable effort may be put into describing excitation modes that do not significantly affect the cable response. Because of the complexities, including interwire coupling, multiple excitation modes, nonlinearities, etc., it does not seem to be possible to identify only dominant processes prior to some code development. The code development we refer to here is primarily one for bookkeeping purposes rather than for solution technique improvement.

A second approach to the problem is to use existing techniques for ordinary EM pickup and to add in an approximate fashion the terms representing the additional SGEMP excitations. In this approach, sensitivity studies are performed by varying the magnitudes of excitations over reasonable bounds to identify important excitation modes. Potential problems with this approach are that significant excitation modes may be neglected or grossly miscalculated and that the results tend to be sensitive to the assumptions (e.g., effective electron ranges, effective gaps, and equivalent capacities).

The approach we have taken in this effort is a combination of the two identified above. Models utilized in both of these approaches are described in the remainder of this document; a description of the efforts along both lines is given in Reference 9.

1.3 REPORT ORGANIZATION

The remainder of this document is devoted to a detailed definition of the problem and an introduction to a number of suitable approximate techniques. The problem is defined in Section 2, and various three- and two-dimensional approximate techniques are introduced. Several approximate techniques for treating the excitation of a shielded single coaxial wire are in Section 3, while similar techniques for an unshielded single wire are discussed in Section 4. An extension of these techniques to multiple-wire bundles is discussed in Section 5. Finally, a summary of the present effort and recommendations for future efforts are given in Section 6.

Appendices A, B, and C include descriptions of selected efforts performed in developing and checking out a computer code to treat the cable response problem.

Volume II contains a description of efforts performed by Mission Research Corporation in support of this effort.

2. PROBLEM DEFINITION

2.1 CABLE DESCRIPTION

Before defining the problem in detail, we give a brief physical description of the types of cables encountered in typical systems. While the application of this effort is not necessarily restricted to SGEMP effects on satellite systems, this is the principal application of the present effort, and therefore, cable systems on a typical satellite (Ref. 10) are described to familiarize the reader with the cable configurations of interest.

Satellite cables are found principally in two or three locations with respect to the satellite structure, as shown in Figure 1 and identified below.

1. Routed on equipment platforms (typically interconnecting boxes).
2. Routed along struts within or external to the structure.
3. Routed on the faces of the solar cell substrate.

The cable harnesses typically consist of three types of cables:

1. Individual insulated wire (similar to hookup wire),
2. Coaxial cables,
3. Shielded multiple wires (two to five wires).

It is quite unlikely that one would find a satellite cable bundle having numerous wires with an overall braid shield, although such a design in the future is not out of the question.

Lengths of cables vary, depending on the dimensions of the satellite. An approximate distribution for the satellite depicted in Figure 1 is shown in Figure 2.

Typical cross sections of the three types of cables indicated above are shown in Figure 3. Both the coaxial cable and shielded pair may have vacuum gaps between the shield and the dielectrics surrounding the wires, which may have a significant effect on the cable response.

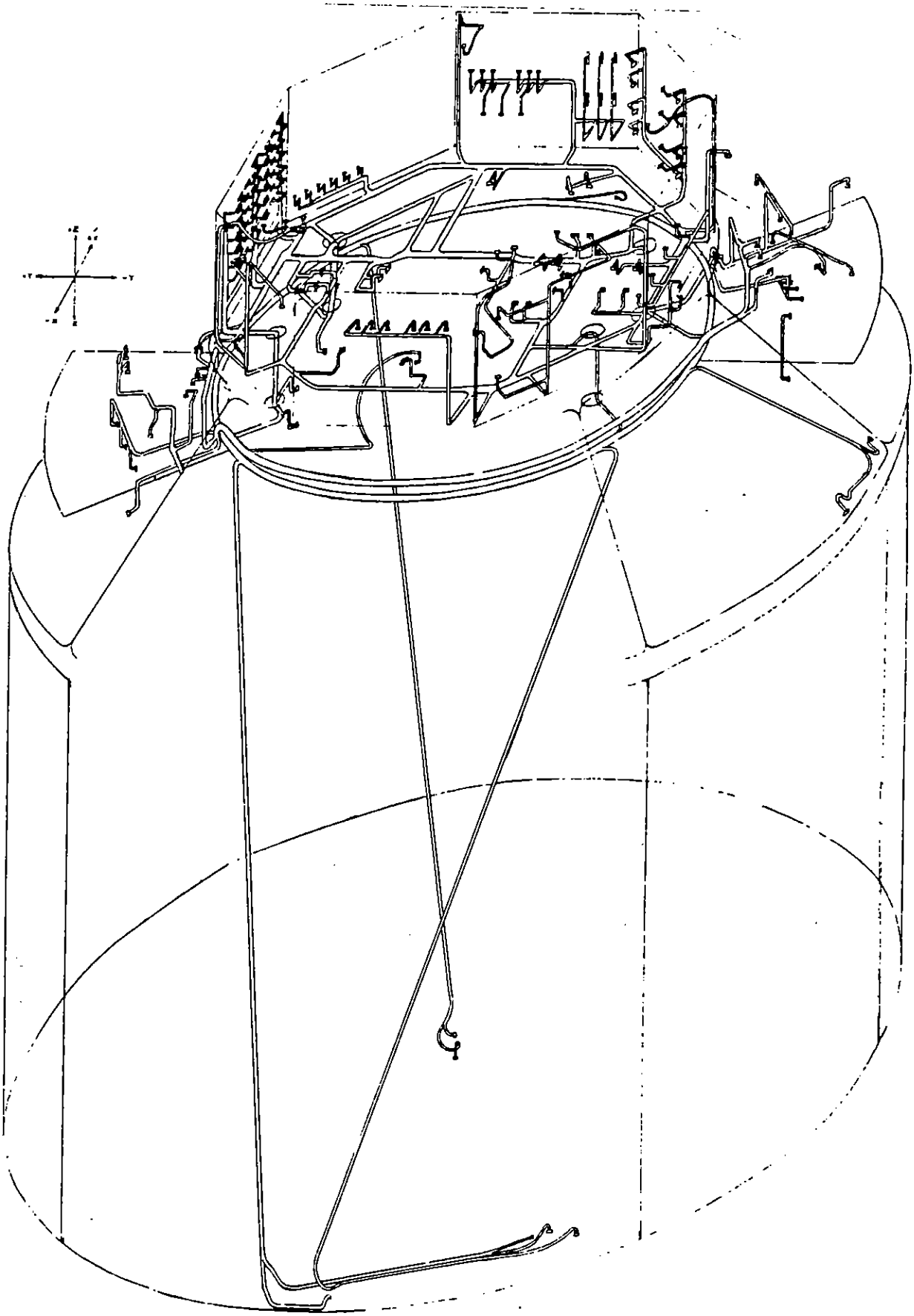

Figure 1. Harness layout in a military spacecraft

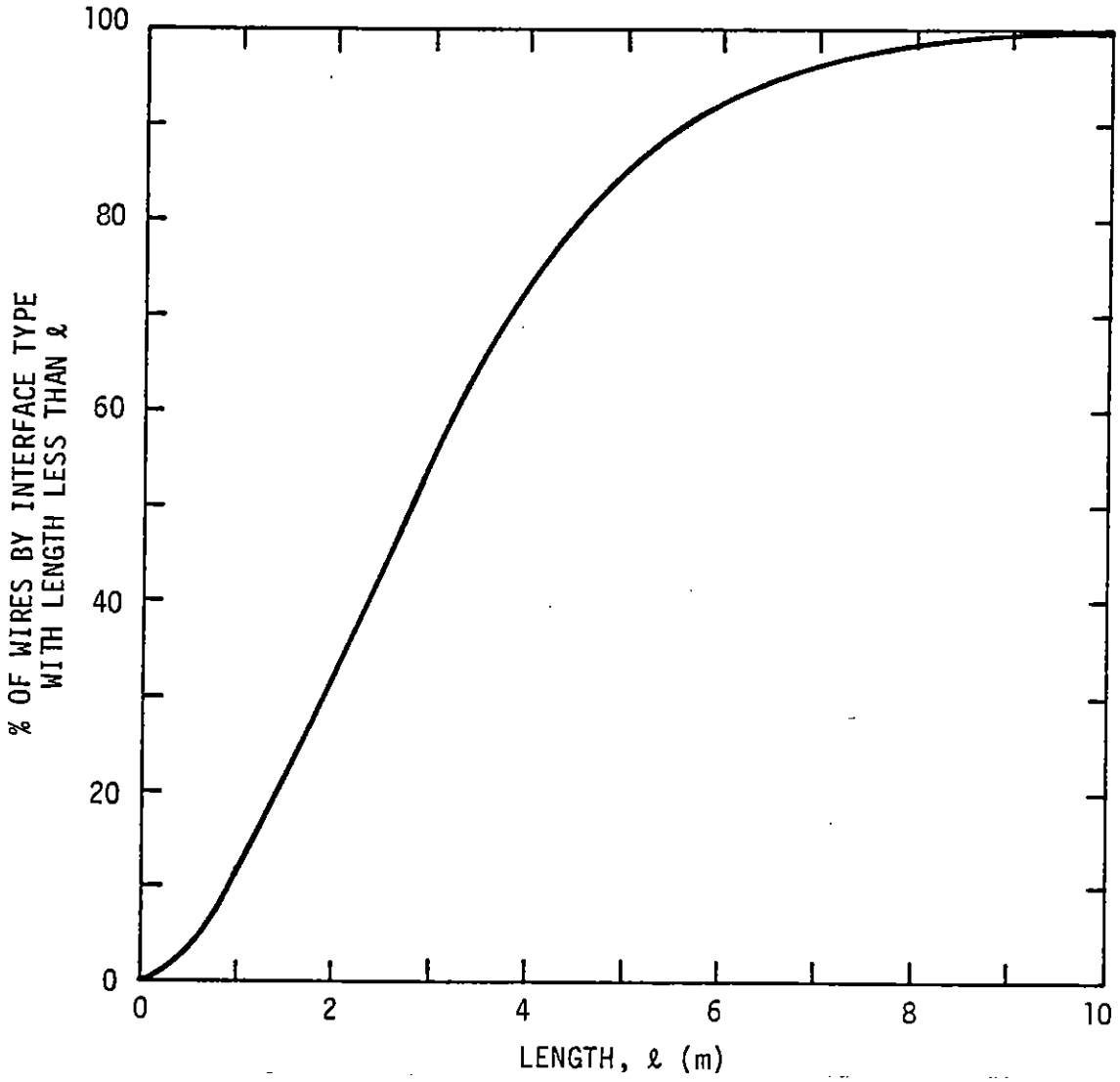

Figure 2. Distribution of wire lengths in satellites; composite of DSP, DSCS II, FLTSATCOM

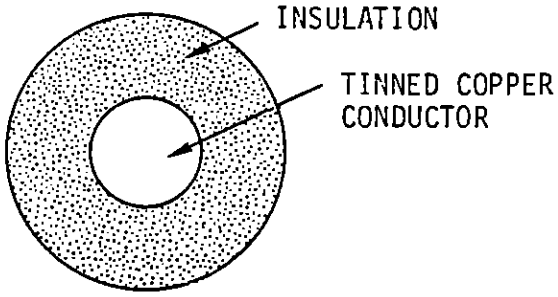

a. Single-wire, #22

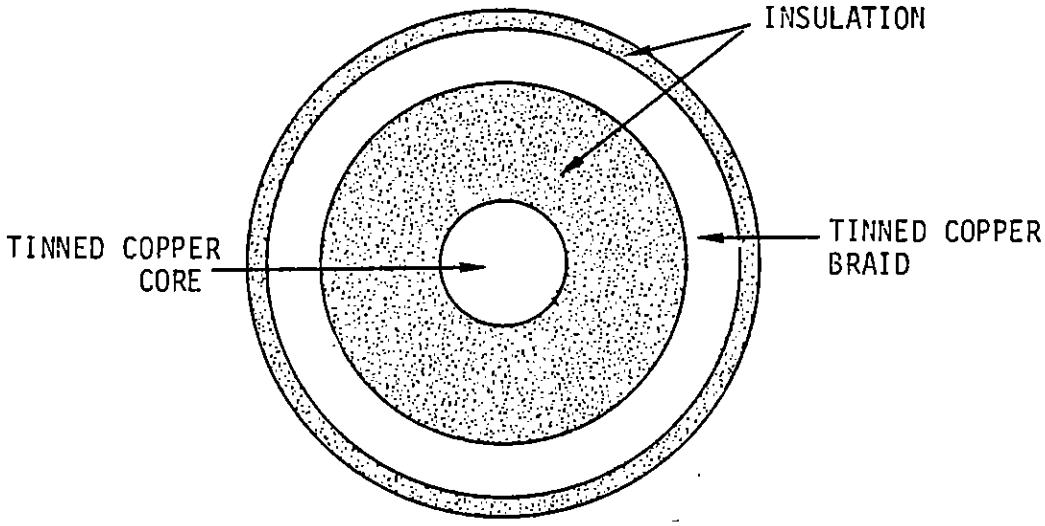

b. Coaxial cable

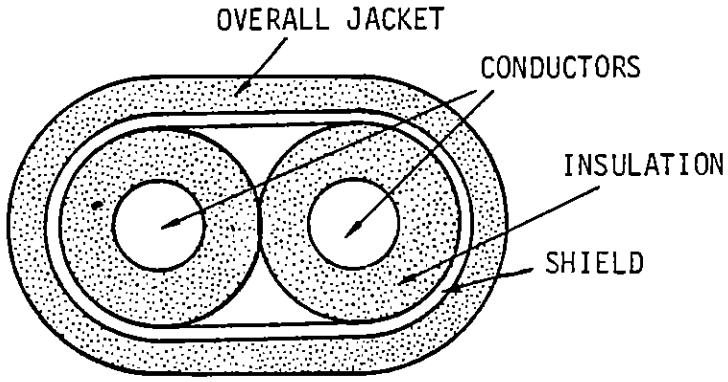

c. Typical pair cross section

Figure 3. Typical cross sections of three types of cables

2.2 PROBLEM DESCRIPTION

The specific problem of interest is that of computing the electromagnetic response of various cable bundles on a complex structure such as a satellite system. This response is produced when incident x rays strike the structure and cables, causing photo-electrons to be emitted. Currents and associated electromagnetic fields are produced that couple into system cables. In addition, photon-induced currents are produced directly within cable bundles, shielded as well as unshielded, by transfer of charge among the various conductors. The entire process is, in general, highly nonlinear due to:

1. Space-charge-limiting effects that alter emitted electron trajectories,
2. Nonlinear circuits that load the cables,
3. Possible breakdown effects on structural elements and cables that carry unusually large current (voltage) pulses.

In principle, the cable problem can be solved with the same SGEMP techniques utilized for the structural response calculations. In fact, the cable harnesses can simply be treated as part of the structure, and the cable response can be computed simultaneously with the structural response.

Unfortunately, this approach is not practical for several reasons. The existing practical SGEMP computer techniques having the capability to treat a two- or three-wire problem in sufficient detail are limited to two-dimensional treatments. However, the cable problem is inherently three-dimensional because of electron trajectory perturbation effects in the plane normal to the wire and propagation effects down the length of the wire. Thus, state-of-the-art tools for practical computer models would have to be extended to full three-dimensional treatments.

Such an extension is within the grasp of existing technology, and this approach may, in fact, be useful and feasible for phenomenology studies of a small number of well controlled wires. This approach may also be useful in verifying more approximate techniques; however, it is not likely that such an approach will ever work for complex systems in which there are a large number of cable harnesses, not to mention the structure itself.

At present, it is difficult (if not impossible) to accurately describe the response of the structure in the absence of cable harnesses. Thus, we are forced to turn to more approximate techniques in which the cable problem is decoupled from the structural problem.

2.3 DECOUPLING ASSUMPTIONS

2.3.1 Structural Response Decoupling

To form a tractable problem, it is necessary to decouple a substantial fraction of the cable response from the structural response. The idea here is to identify all those cables which could be removed from the structure without substantially perturbing the "gross" structural response in terms of charge and current distributions and associated fields. Local field and current perturbations in the vicinity of the cabling are permissible and are not considered to be gross structural response perturbations.

Cables that cannot be decoupled from the structure are primarily those which interconnect otherwise isolated structural elements such as floating equipment boxes or compartments. Whether the cable can be decoupled is primarily a question of (1) how much structural replacement flows as a result of electrons emitted from the structure to which the box is connected, and (2) how much of this replacement current flows through the cable versus the structure.

The separation of these cables in a complex system is, of course, difficult, and one may eventually have to appeal to experimental results to verify that such a decoupling process is possible. This separation question can be treated analytically, to a limited extent, by comparing predicted structural responses with and without the cable present.

If the cables are properly decoupled, the following prescription can be followed.

1. The few cables with large structural replacement currents are treated as part of the structure; these cables will produce significant local fields that may couple into other cables.

2. The preponderance of cables with small structural replacement currents are primarily excited by local electric and magnetic fields and currents, and the excitation of these cables can be effectively decoupled from the structural response.

Some cables will not fall into either category; there will always be cables which are excited almost equally by structural replacement flow and by local fields and currents.

2.3.2 Shielded Cable Decoupling

A second group of cables, whose excitation can readily be decoupled from the remainder of the system, are those that are "well shielded" from EM pickup external to the cable shield. By "well shielded" we mean those cables whose photon-induced excitation* within the cable shield greatly exceeds the response induced by leakage of currents flowing on the shield. In practice, this category covers a wide variety of modest shielding configurations that can, in some cases, include even relatively poor schemes, such as short pigtailing at the connectors.

The photon-induced response of these cables is certainly, to the first order, decoupled from the system and can be analyzed independently from the number of cables forming the bundle, the structural location, etc. Estimates of leakage currents through shields using transfer impedance concepts (Ref. 11) can be utilized to ensure that photon-induced currents within the cables are dominant.

2.4 THREE-DIMENSIONAL APPROXIMATIONS

It was pointed out in Section 2.2 that the cable excitation problem can be rigorously treated by modeling the system cable and structure as one coupled unit. It was also pointed out that such an approach leads to an intractable problem for cables composed of anything other than simple bulk cables, and that decoupling approximations are required to treat more

*Transfer of charge between wires and between the shield and wires.

complex cables. Even when the problem is decoupled, additional computational technique development is required to treat the system in the three-dimensional space needed to describe the problem.

In this section, we consider the solution technique required to rigorously compute the excitation of a cable for which the structural decoupling is assumed to be valid. The simple case of a cable bundle connecting two boxes laying on a ground plane is considered first. Comments are made about the extension of this technique to treat cables with breakouts leading to other boxes.

2.4.1 Cables over a Ground Plane

As a starting point for computing the excitation of the decoupled cable, we assume that SGEMP excitation has been obtained for the structure in the absence of the cable harness. Thus, the electric and magnetic fields and electron current densities unperturbed by the cables are assumed to be known along the ground plane and at some arbitrary and imaginary surface enclosing the cable and boxes, as shown in Figure 4. The imaginary

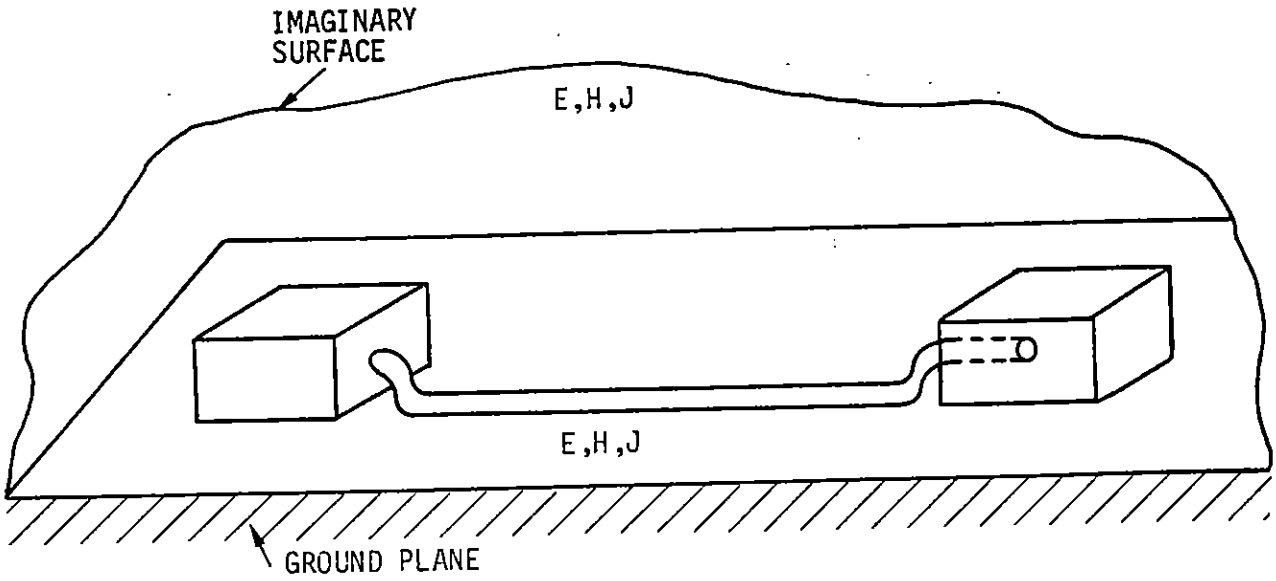

Figure 4. Cable configuration for a single harness over a ground plane connecting two boxes. Unperturbed electric and magnetic fields and electron currents are assumed to be known along the ground plane and at an arbitrary surface enclosing the volume.

surface is chosen to be far enough from the cable harness that the fields and current densities will be essentially unperturbed from their values in the absence of the cables. The cables are attached at the box with an arbitrary resistance load. In principle, complex loads can also be attached. The problem specification is now complete and can, in principle, be solved by using the three-dimensional SGEMP particle-pusher codes using the finite-difference or lumped-element model representation.

The only remaining question is the validity of the perturbation approximation employed. The approximation solution described above can be checked by comparing the unperturbed solution obtained with and without the cable present. If the perturbed solution is valid, the current and field distribution should asymptotically approach each other far before reaching the imaginary bounding surface, as shown in Figure 5.

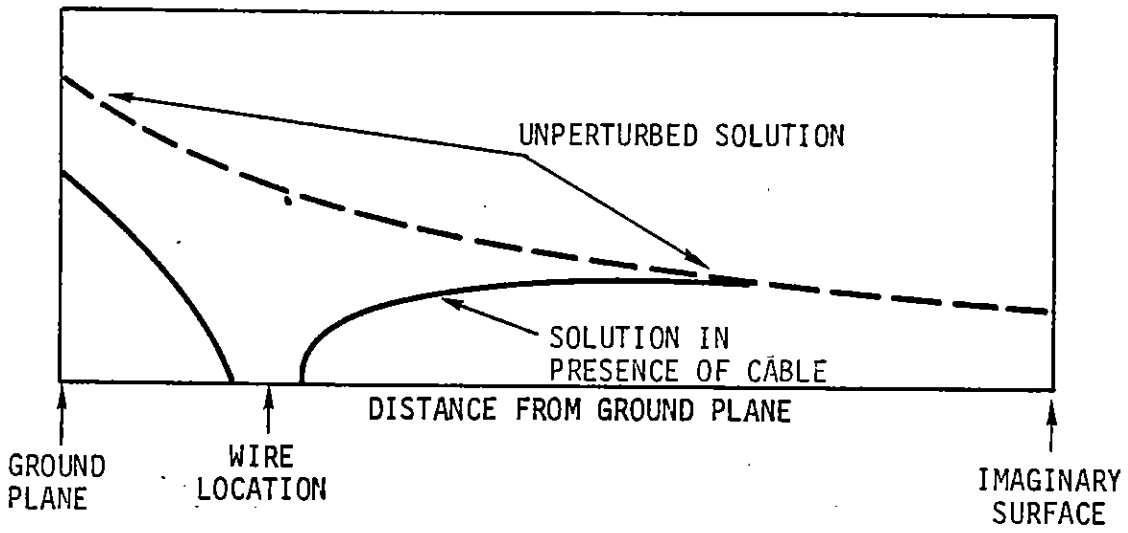

Figure 5. Check on accuracy of decoupling approximation requires a comparison of solutions obtained with and without cables present.

2.4.2 Cable Breakouts

The configuration described in the previous chapter is suitable for situations in which cables run between only two boxes. In practice, most cable harnesses have numerous cable breakouts.

The most obvious approach to this problem is to include a third cable and box within the bounding surface. This may, of course, be done with increasing difficulty for one or two breakouts, but the extension of this technique to all breakouts leads to solving the entire cable harness and structure as a coupled system.

Another approach is to let the cable pass through the bounding surface, as shown in Figure 6. The unperturbed electric and magnetic fields and

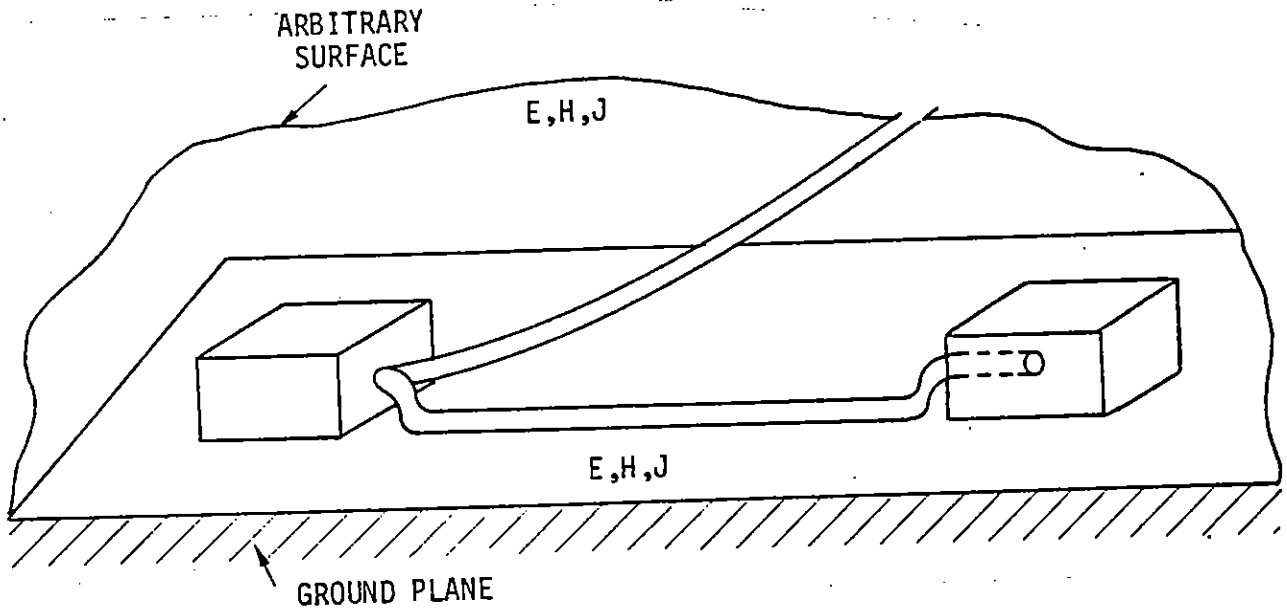

Figure 6. Cable system with single breakout

currents on the bounding surface are again assumed to be known in the absence of cabling. However, the fields and currents at the imaginary surface are strongly perturbed in the region through which the cable passes regardless of where the cable is placed. Also, there is no good way to treat the cable section and cable load on the section outside the region. An approximate technique could be developed by assuming some

type of local boundary condition in terms of local fields and cable currents at the point where the cable passes through the imaginary surface, but the solution within the bounding region in general depends upon the local cable voltage which, in turn, depends upon the excitation of the cable in the region outside the boundary.

Because of the problem of cable breakouts and the problem of increasing complexity with several coupled cable bundles, it appears that investigations into other, more simplified techniques is warranted, particularly if they are to be applicable to system studies. In the next section, we describe two-dimensional techniques which permit approximate solutions with more complex bundles.

2.5 TWO-DIMENSIONAL APPROXIMATIONS

2.5.1 Transmission-Line Model Validity

We have stated that the cable problem is inherently three dimensional because (1) the cable excitation described by electric and magnetic fields and corresponding electron trajectory perturbations must be considered, at a minimum, in the two-dimensional plane perpendicular to the cable, and (2) propagation effects must be considered in a third direction down the length of the cable.

The problem can be greatly simplified if the cables can be represented by a transmission-line model so that excitation source terms per unit length can be computed on a two-dimensional basis and propagation effects can be considered by utilizing a set of coupled transmission equations. Should such a technique prove feasible, an entire set of coupled system cables could be represented by a tractable model.

The requirements for the validity of a transmission-line model are that pertinent wavelengths of signal cables be large with respect to pertinent transverse cable distances. For problems of interest in SGEMP, this approximation is valid for virtually all shielded cables and for all cables laying near ground planes. Pertinent frequencies of interest are generally always less than 10^9 Hz, and therefore, transverse cable distances must be less than $\lambda = c/f = 0.3$ m. Thus, the transmission-line approximation should be valid for most satellite system cables. One notable

exception may be cables routed on thin struts which, in turn, are located some distance away from a conducting satellite surface. A second potential exception is cable harnesses routed over imperfect conducting planes such as honeycomb substrates. However, the limited measurements to date, using bounded-wave excitation sources, indicate that the response of cables over a honeycomb plane closely resemble the response of the same cable over a good conducting plane. A third potential problem may arise when cables pass over several conducting planes which are detached, or isolated, from each other, such as when cables pass from the solar array substrate to equipment platforms.

It is beyond the scope of this effort to rigorously justify the transmission-line approximation for all conceivable cable situations in satellites. Suffice to say that we believe that the transmission-line model is valid for at least a large fraction of the satellite cables and that detailed and rigorous justification must await experimental results and/or development of the techniques described in the previous section, so comparisons can be made to results obtained with the transmission-line model.

We choose to represent the transmission line by a set of lumped parameters per unit length, as shown in Figure 7, where L and C are

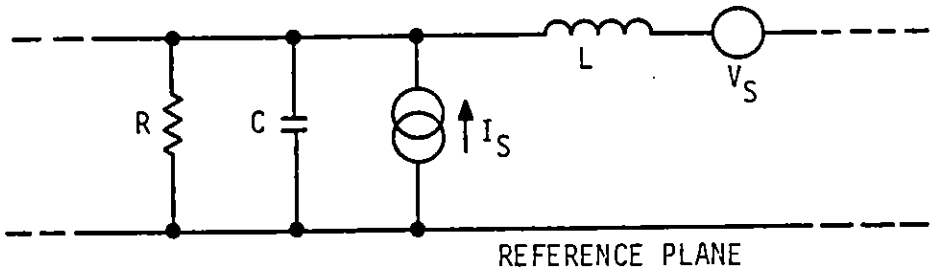

Figure 7. Transmission-line model representation per unit length

the inductance and capacitance per unit length, R is the shunt impedance per unit length caused by radiation-induced conductivity in surrounding dielectrics if any, and V_S and I_S are voltage and current sources per unit

length used to describe the cable excitation. The reference plane is the shield of a shielded cable bundle or the ground plane under an unshielded bundle. One set of these elements is used to represent each wire in a bundle; in addition, mutual capacity, inductance, resistance, and excitation sources between each two sections are also utilized, although they are not specifically shown in Figure 7.

This model is rather standard for use in predicting excitation by EMP environments (Ref. 12) and should not require further description. The problem with which we are concerned here is one of modeling and describing the source terms applicable to SGEMP excitation. In the following section, we qualitatively describe the sources of excitation in the SGEMP environment and the computational difficulties involved in quantifying these sources.

2.5.2 Excitation Sources

The transmission line is described by a number of cable parameters and excitation sources per unit length. These lengths are chosen to be short relative both to pertinent wavelengths and to pertinent spatial grandients of fields. Thus, it is assumed that the excitation sources can be computed by solving a two-dimensional problem in a plane perpendicular to the cable length.

A necessary ingredient for the validity of the transmission-line approximation is that potential differences between the reference plane and the wires be well defined and independent of path (within a plane perpendicular to the wires). This assumption, along with the assumption that there is no change in the potential along the length of each segment of the transmission line, is equivalent to assuming that the local electric field is irrotational ($\nabla \times \vec{E} = 0$). This condition is precisely that required for the applicability of the quasi-static approximation. We consider this fact to be an important result and wish to emphasize here (1) that to compute the source terms per unit length for SGEMP excitation in the transmission-line approximation, the quasi-static approximation is sufficient, and (2) that in fact, if the results of a fully dynamic treatment were substantially different from the quasi-static solution in the vicinity of the cable, the entire transmission-line approach would be invalid.

The method by which the source terms per unit length for the transmission-line model can be computed is illustrated with the simple cable located above a ground plane in Figure 8. Once again, the

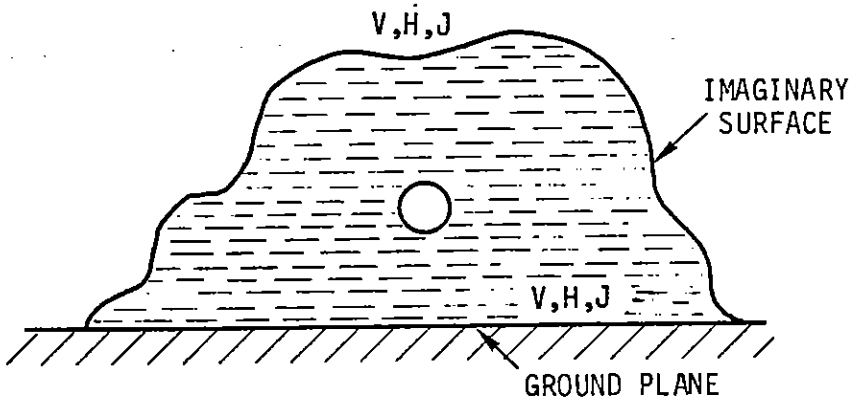

Figure 8. Two-dimensional representation of cable used to compute source terms per unit length

imaginary surface is placed sufficiently far from the cable that the field at the boundary is not perturbed by the presence of the cable. The unperturbed potential V along the imaginary boundary, the magnetic fields, and the current densities are assumed to have been computed from the structural response model in the absence of the cable.

The two-dimensional problem shown in Figure 8 can now be solved to obtain the source terms. Excitation terms arise from the following sources.

1. The changing potential on the boundary. This source actually represents the contribution from the electric field produced in the remainder of the system.
2. The charge within the volume, which is, in turn, producing a changing electric field across the cable. The contribution from this term is similar to the one described above and need be separated only when significant perturbation in the

local charge location surrounding cable occurs (e.g., high space-charge-limiting). The local problem is separated to form a tractable problem. In the absence of such a perturbation, the two sources can be combined and the excitation is then produced by the unperturbed potential.

3. The net charge deposited onto the conduction surface (charge striking the cable from the boundary cables, etc., minus the charge emitted from the cable).
4. The changing magnetic field. In the approximate treatment described here, the magnetic field is assumed to be unperturbed by the presence of the cable.* Large perturbations in incident magnetic fields at the arbitrary boundary would indicate the cable carries a significant fraction of structural current, in violation of the small perturbation assumption.

For several reasons, it is important to distinguish between each of these sources and to identify those which are most effective in producing response currents:

1. Sources which do not significantly contribute may be eliminated, thus simplifying the computation.
2. Different sources of excitation have different uncertainties associated with them.

In the following three sections, we give more detailed descriptions of of several approximate techniques that can be used to model and quantify each of these source terms. Consideration is given to both unshielded and shielded wire bundles. We consider a single shielded wire first because we need not consider contributions from electric and magnetic fields generated by the remainder of the structure.

*More precisely, we mean that the cable excitation from the magnetic field is computed by considering the incident field and ignoring the scattered field. Measurements indicate that such an approach is valid for cables located a short distance over good conducting ground planes.

3. SHIELDED CABLES

In this section we consider the excitation of a single wire surrounded by an integral electrical shield. The shielding effectiveness is assumed to be sufficient to ensure that the decoupling assumption is valid, thus, the problem of excitation from the photon-induced charge transfer within the cable is assumed to be separable from the problem of external shield current excitation. Of course, the contribution from leakage of external currents can be added, if required, by utilizing transfer impedance concepts or by direct use of data from current-injection excitation of the outer shield. Generally, the photon-induced currents within the cable dominate over leakage currents for cable shields having even minimal integrity.

3.1 COAXIAL CABLE

The coaxial cable configuration is by far the simplest configuration to treat theoretically because of the inherent cable symmetry. The photon excitation of such a cable is a result of charge transfer between the center conductor and the outer conducting shield. Because of the intervening dielectric and the fact that virtually all electron ranges of practical interest are small relative to the dielectric spacing, there is no direct charge transfer between the two cables in the sense that electrons emitted from one conducting surface strike the other conducting surface. Rather, the excitation is produced by displacement currents which, in turn, arise from charge accumulating in various regions of the dielectric.

These sources of excitation can be conveniently divided into three categories:

1. Charge accumulation at the interface between the outer shield and the dielectric, arising from charge emission efficiencies which, in general, are different for the two different materials.

2. Charge accumulation at the dielectric-core interface for the same reason stated above.
3. Charge accumulation in the dielectric bulk arising from the attenuation of the photon flux passing through the dielectric. The attenuation causes a divergence in current which results in accumulation of charge throughout the dielectric.

These three source regions are shown schematically in Figure 9. In creating this schematic, we have tacitly made the following assumptions.

1. The electron ranges are short relative to the dielectric thickness.
2. The emission efficiency of the conductor is higher than that of the dielectric, resulting in net accumulation of negative charge within the dielectric near both interfaces.

It is important to distinguish from which conducting surface each electron in the dielectric was effectively emitted. More precisely, it is necessary to know, for each charge in the dielectric, whether the image charge for the open-circuit cable resides on the shield or on the core. Those charges whose image lays on the core produce cable currents of opposite sign compared to those whose image resides on the shield.

The regions of charge within the dielectric are divided into two classes in Figure 10, one corresponding to those whose image resides on the core and another for those whose image resides on the shield. The importance of distinguishing between these sources will become evident in the following sections where specific calculations for coaxial cables are illustrated.

3.1.1 Excitation Sources for a Coaxial Cable

The fundamental problem is to define a source term per unit length that represents the excitation produced by a charge accumulating at a single point in the dielectric. Source terms for all other charges can then be computed in a similar fashion by direct summation or integration.

Consider a time-dependent charge $q_0(t)$ emitted from the outer shield coming to rest at radius r_0 located an electron range r_e from the outer

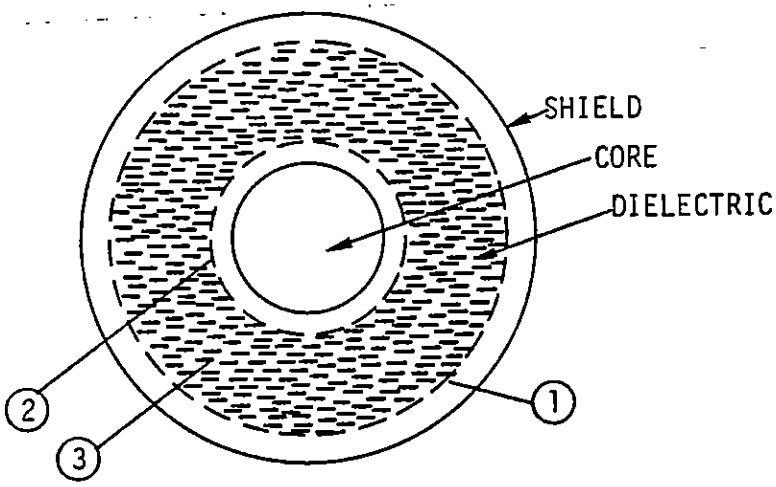

Figure 9. Schematic cable cross section illustrating three source regions of cable excitation corresponding to accumulation of charge (1) at the shield-dielectric interface, (2) at the core-dielectric interface, and (3) in the dielectric bulk

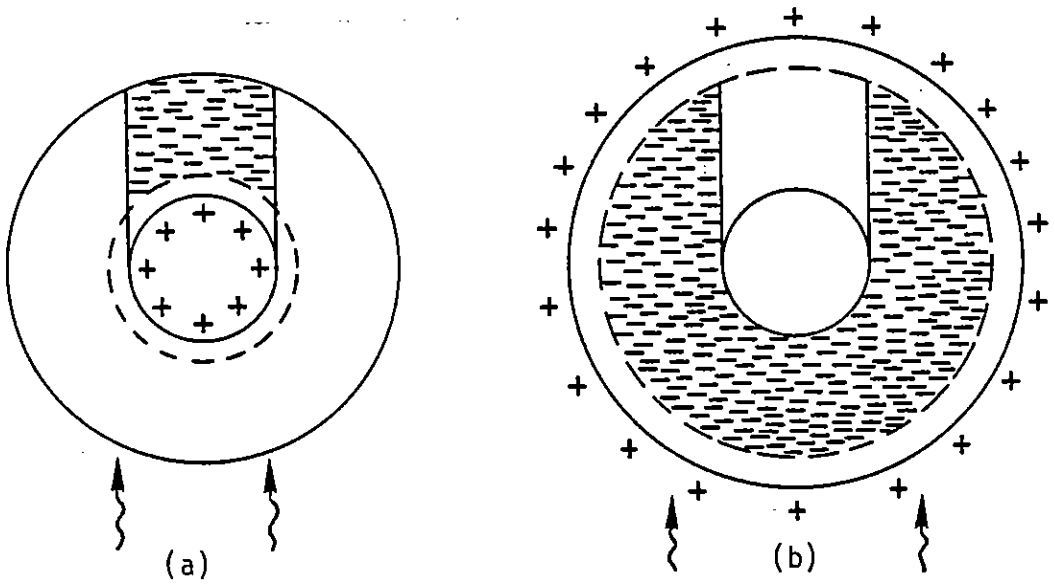

Figure 10. Schematic of charge whose image is (a) on the core and (b) on the shield

conductor, as shown in Figure 11. The excitation source term per unit length can be determined directly from the open-circuit voltage produced between the outer and inner conductors:

$$I = \frac{C\, dV_{OC}}{dt} , \tag{3-1}$$

where C is the capacitance between the center and outer conductors,

$$\frac{1}{C} = \frac{1}{2\pi\varepsilon} \ln \frac{r_2}{r_1}$$

The corresponding transmission-line model per unit length is shown in Figure 12, along with the current source I.

The remaining problem is to compute $\dot{V}_{OC}$ in terms of the charge $q_0(t)$ and the radius r_0. This can be accomplished by solving Poisson's equation either numerically or analytically. The coaxial configuration is particularly amenable to an analytical solution, as outlined below.

From symmetry considerations, the open-circuit voltage induced by a point charge $q_0(t)$ at radius r_0 is identical to the voltage induced as if the charge were uniformly spread out along a concentric circle at radius r_0. The fact that the angular location has no effect on the cable excitation is significant because it means that uncertainties in the magnitude of charge as a function of angle at a fixed radius do not contribute to uncertainties in response predictions.

The equivalent problem (insofar as the open-circuit voltage is concerned) possesses cylindrical symmetry, and the open-circuit voltage is simply

$$V_{OC}(t) = \frac{1}{2\pi\varepsilon} \ln \frac{r_2}{r_0} = \frac{q_0(t)}{C_0} , \tag{3-3}$$

where C_0 is the capacity between the shield at radius r_2 and an imaginary conducting surface at r_0 (see Figure 11).

An alternate equivalent circuit can be formed in which the current source is expressed directly in terms of the charge $q_0(t)$. An equivalent circuit of Figure 12 is shown in Figure 13 in which the current source $q_0(t)$ is placed directly between the outer shield and the imaginary

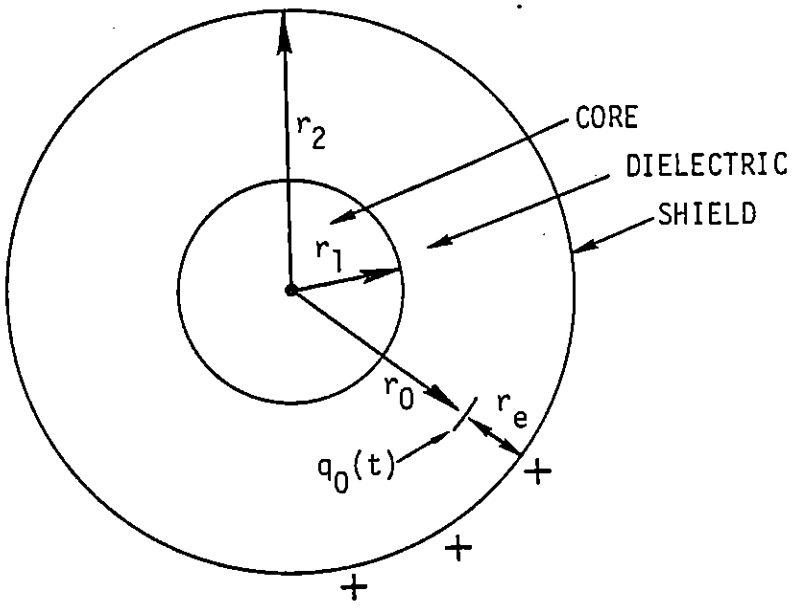

Figure 11. Charge $q_0(t)$ located at radius r_0 with an equivalent image charge $-q_0(t)$ located on the shield

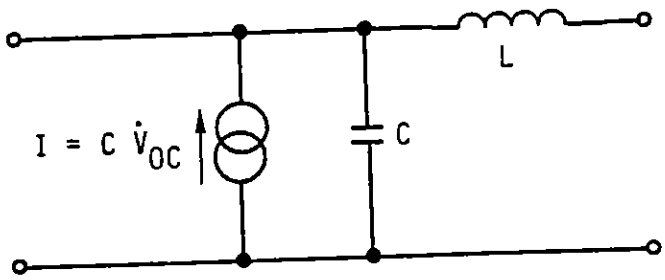

Figure 12. Transmission-line model for a coaxial cable excited by a charge $q_0(t)$ producing an open-circuit voltage V_{OC}

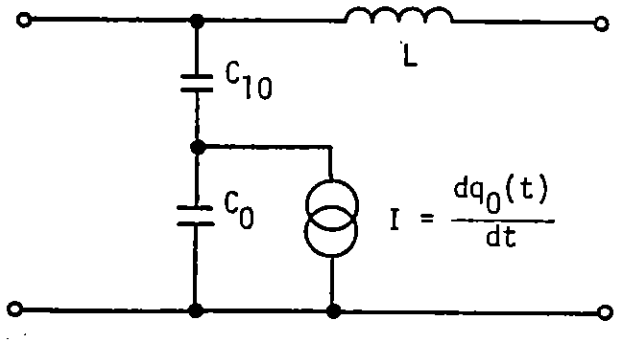

Figure 13. Equivalent circuit of Figure 12 in which the current source is explicitly represented by $dq_0(t)/dt$ rather than by $\dot{V}_{OC}$

conducting surface at radius r_0. The capacity C_0 represents the capacity between the imaginary surface at radius r_0 and the inner conductor of radius r_1. The combined series capacity of C_{10} and C_0, of course, equals the total capacity C between the shield and the core:

$$\frac{1}{C} = \frac{1}{C_{10}} + \frac{1}{C_0} .$$

We now consider an additional charge $q_i(t)$ emitted from the inner wire towards the outer wire located at radius r_i such that the image charge resides on the core. The equivalent circuit for this case is shown in Figure 14, where C_{i0} is the capacity between two imaginary surfaces at r_i and r_0.

It is evident that this form of the equivalent circuit is not convenient for computational purposes because one capacitor is required for each radius at which charge is located. A more convenient form of the equivalent circuit is that shown in Figure 12, where the source term is now

$$I = C\,\dot{V}_{OC} = C \sum_0 \frac{q_0(t)}{C_0} - C \sum_i \frac{q_i(t)}{C_i} . \qquad (3\text{-}4)$$

The various charges q_0 are located at radii r_0 with images in the shield, while the various charges q_i are located at radii r_i with images in the center core.

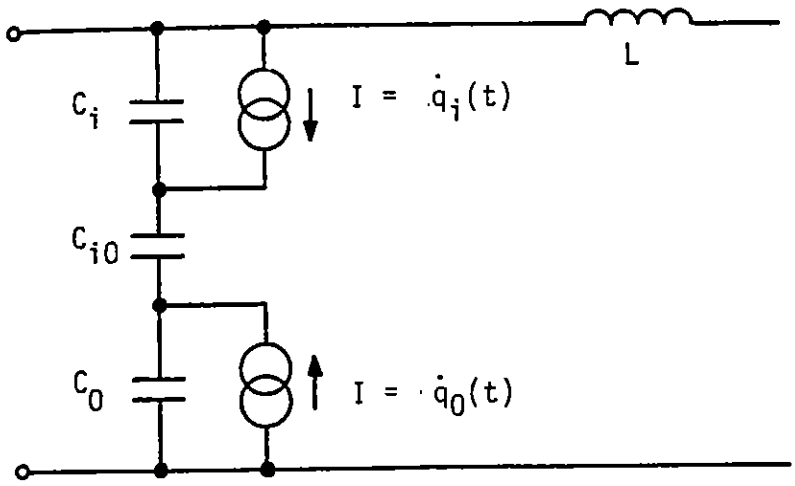

Figure 14. Equivalent circuit for charge $q_i(t)$ residing at r_i with an image charge $-q_i(t)$ on the core, and charge $q_0(t)$ residing at r_0 with an image charge $-q_0(t)$ on the shield

3.1.2 Vacuum Gaps

The coaxial cable may have vacuum gaps between the shield or core and the dielectric. Gaps larger than an electron range can significantly affect the cable response by allowing charge emitted from the core or shield to travel a significantly greater fraction of the distance between the conductors. The equivalent circuit for gaps at both conductor-dielectric interfaces is shown in Figure 15.

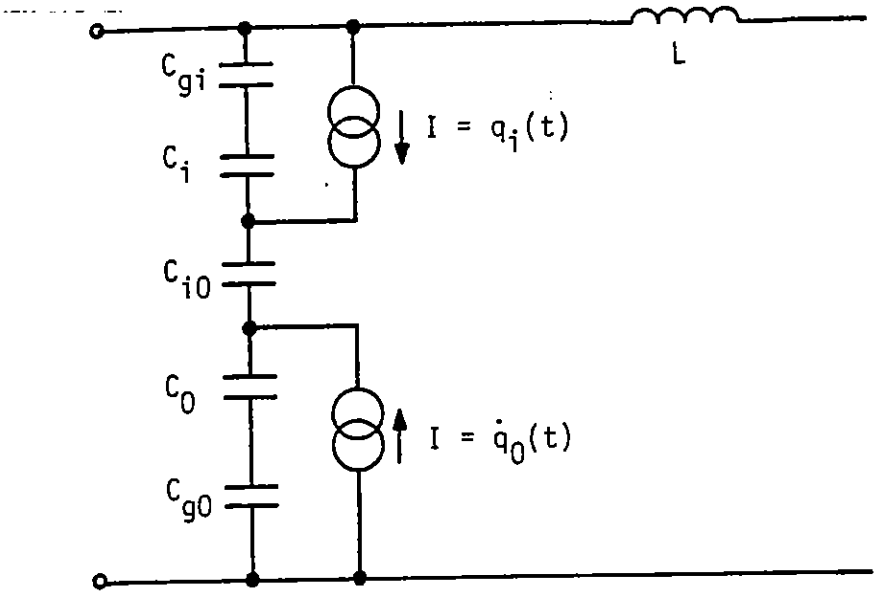

Figure 15. Equivalent circuit for gaps located between the shield and dielectric and between the core and dielectric

3.1.3 Practical Considerations

In the previous subsections, solutions have been obtained for known charges at given locations. We now address the practical problems associated with computing the complex charge distribution in the dielectric.

The most rigorous approach is to perform photon attenuation and electron transport calculations utilizing a two-dimensional numerical solution technique. In this way, the charge accumulation at both conductor-dielectric interfaces and within the dielectric bulk can be accurately computed. The charge at each radial position r_i (having image charge in the core) and r_0 (having image charge in the shield) is summed over angle Θ, and the equivalent source term I per unit length is accurately computed by summing over radial positions using Eq. 3-4.

We now turn to more approximate techniques that do not require repeated 2-D computations. The general approach is to define effective ranges at which the equivalent amounts of charges may be placed to produce a response equal to that produced by the distribution. The effective radii can be parametrized in terms of cable diameter, insulation thickness, electron energy, etc.

In the following paragraphs, we outline a simplified approach which may find utility in cable response calculations. Of course, any approximate technique should be validated, perhaps by comparing with the complete 2-D solutions. The cable is broken into six segments for purposes of electron transport calculations, as shown in Figure 16. Photon transport and electron emission calculations are performed along two ray paths, one essentially through the center of the cable and one at some radius which produces an average or "effective" amount of charge in the bulk and at the interfaces. Computations required along each path length are forward and reverse emission at each dielectric-conductor interface. Consideration must be given to the attenuation of the photons by the cable shield, dielectric, and core as well as by the surrounding system before photon entry into the cable.

Effective radii must be found at each of the six interface locations numbered 1 through 6 in Figure 16. In addition, equivalent radii must

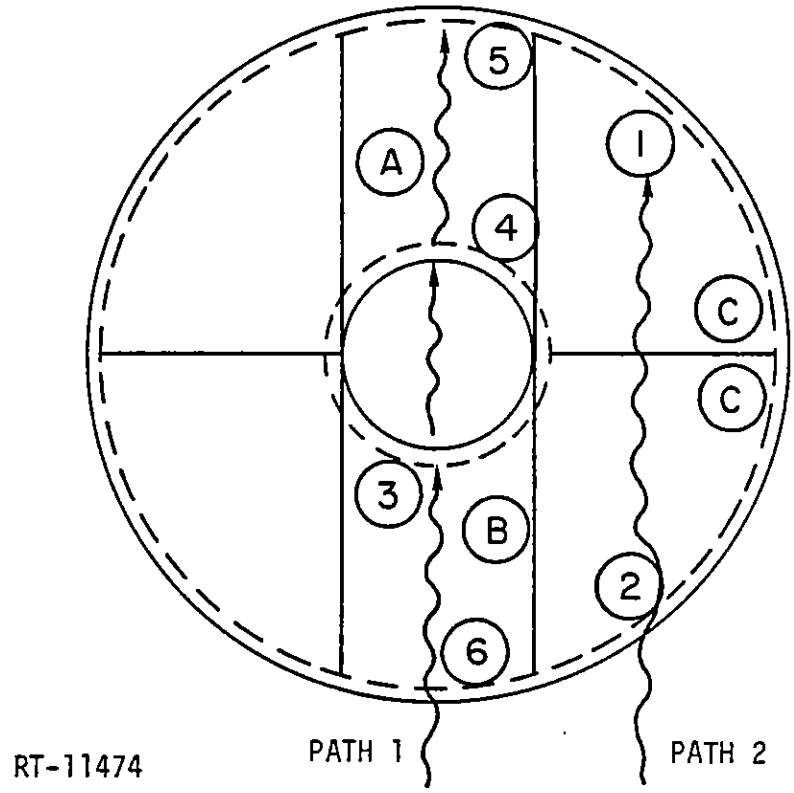

Figure 16. Division of cable for photon attenuation and electron emission calculations

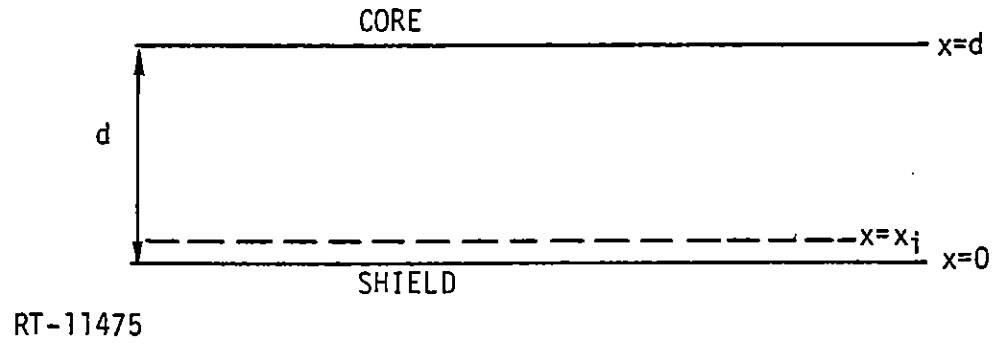

Figure 17. Planar approximation to a cable section

be found for the charge in the bulk in each of the three regions lettered A, B, and C. The effective radii can be defined in a number of ways; we illustrate one method using a planar approximation for each region.

As an example, consider a planar approximation to one section of the cable as shown in Figure 17. The open-circuit time derivative of voltage produced by a current element J_i, containing electrons with an energy range such that they deposited at a layer x_i, is

$$\dot{V}_{OC}^{i} = \frac{J_i\, x_i}{\varepsilon} . \tag{3-5}$$

The open-circuit voltage for all such current elements is

$$\dot{V}_{OC} = \sum_i \frac{J_i\, x_i}{\varepsilon} . \tag{3-6}$$

The effective range $\langle r_e \rangle$ is found by computing the potential produced by placing all current elements at $\langle r_e \rangle$ and equating this value to $\dot{V}_{OC}$:

$$\sum_i \frac{J_i\, x_i}{\varepsilon} = \frac{\langle r_e \rangle \sum J_i}{\varepsilon}$$

or

$$\langle r_e \rangle = \frac{\sum J_i\, x_i}{\sum J_i} . \tag{3-7}$$

A similar approach may be taken for charge deposited within the bulk. In this case, the partial current is given by $J_p(x) = J_p \exp(-x/\lambda_p)$, where the subscript p refers to photons of energy p. As before, the total net current* may be found by summing over p. The charge density is $\partial\rho/\partial t = -\nabla \cdot J$. The resulting open-circuit voltage change is

$$\dot{V}_{OC}^{p} = \frac{J_p}{\varepsilon} (d - \lambda_p) \exp(-d/\lambda_p) + \frac{J_p}{\varepsilon} \lambda_p . \tag{3-8}$$

As before, we equate the value to the potential produced by an equivalent charge at an effective distance $\langle x \rangle$:

$$\dot{V}_{OC} = \langle x \rangle \sum_p \frac{J_p}{\varepsilon} = \sum_p \left[\frac{J_p}{\varepsilon} (d - \lambda_p) \exp(-d/\lambda_p + \frac{J_p}{\varepsilon} \lambda_p \right]$$

*Net current referring to that which crosses an imaginary plane in the forward direction; i.e., forward minus reverse.

or

$$\langle x \rangle = \frac{\sum [J_p (d - \lambda_p) \exp(-d/\lambda_p) + J_p \lambda_p]}{\sum_p J_p} \quad . \tag{3-9}$$

For cases where $\lambda_p >> d$,

$$\langle x \rangle = \frac{\sum J_p (d^2/2\lambda_p)}{\sum J_p} \qquad (\lambda_p >> d) \ , \tag{3-10}$$

corresponding to small attenuation through the dielectric.

We now use Eqs. 3-5 and 3-8 to compare the contribution to the cable response from the charge accumulation at the interface to the charge accumulation in the bulk of the dielectric. Comparisons are made for photon/electron combinations of 10 and 50 keV. Pertinent parameters are given in Table 1. The shield is assumed to consist of copper, while the dielectric is assumed to have properties similar to carbon.

Table 1

PERTINENT PARAMETERS FOR CABLE EXCITATION COMPARISON
(Electron and photon ranges shown are those for carbon.)

Parameter	10 keV	50 keV
J_{Cu}/J_C	70	150
λ_e (cm)	1.26×10^{-4}	4.8×10^{-3}
λ_p (cm)	2.12×10^{-1}	5.6

The emission efficiency of the copper is significantly higher than that of carbon, so that the charge accumulations at the interfaces are assumed to be characteristic of emission from copper only. The dielectric thickness d is assumed to be 0.2 cm for purposes of this illustration. Equations 3-5 and 3-8 are used to compute the ratio of contributions to V_{OC} from the accumulation in the bulk to that of the interface. The

current J_i is essentially that from copper because the relative emission from carbon is extremely low. The current density J_p in Eq. 3-8 corresponds to that in the dielectric, carbon for this example. The ratio of contributions from the interface to that of the bulk becomes

$$\frac{\dot{V}_{OC_{interface}}}{\dot{V}_{OC_{bulk}}} = \frac{J_{Cu}}{J_C}\left[\frac{\lambda_e}{(d - \lambda_p)\exp(-d/\lambda_p + \lambda_p)}\right].$$

Results are shown in Table 2.

Table 2

RATIOS OF CONTRIBUTION TO CABLE EXCITATION FROM ELECTRON ACCUMULATION AT THE INTERFACE TO THAT AT THE BULK

Energy	Ratio $\frac{\dot{V}_{OC_{interface}}}{\dot{V}_{OC_{bulk}}}$
10 keV	4.3×10^{-2}
50 keV	0.86

It is evident from these simplistic estimates that the contribution from charge accumulating in the bulk due to photon attenuation is as important as the charge accumulating at the interface due to different emission efficiencies. It is also evident that the contribution from the bulk becomes less important at higher energies, where the photon attenuation is significantly less. The important point here is that contributions from both sources must be included when modeling cables for low-energy x-ray excitation.

4. UNSHIELDED CABLES

Several approximate techniques are described in this section for computing the excitation terms for two cable types:

1. single-conductor, and
2. single-conductor surrounded by a dielectric insulator.

Consideration is given to both self-consistent and non-self-consistent computational techniques.

4.1 NON-SELF-CONSISTENT SOLUTIONS FOR A SINGLE CONDUCTOR

It is assumed here, as previously, that the electric and magnetic fields have been computed in the absence of the cable, and that the potential is known along the arbitrary surface, as shown in Figure 18. The problem we address here is how to compute the source terms per unit length for the transmission-line model shown in Figure 19.

The voltage source is computed by using the unperturbed magnetic field threading the cable:

$$V_S = \int_S \dot{\vec{B}} \, d\vec{A} \ ,$$

where the area of integration lies between the wire and ground plane. This treatment is equivalent to assuming that the scattered magnetic field is small relative to the incident field, an approximation that seems justified for cables over good conducting surfaces.

We now turn to the problem of defining the current source. Three approximate techniques are described below.

4.1.1 Solution Technique 1

The most straightforward method of computing the current source is to solve the problem described by the configuration and boundary conditions

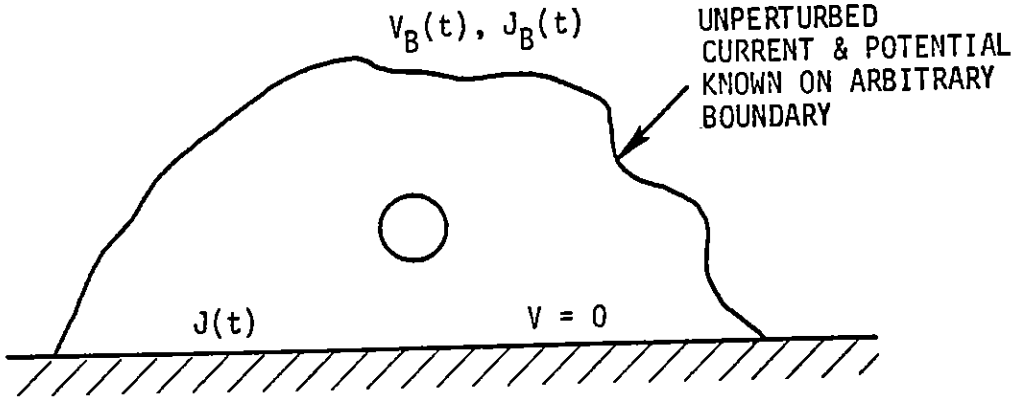

Figure 18. Configuration for a single wire over a ground plane

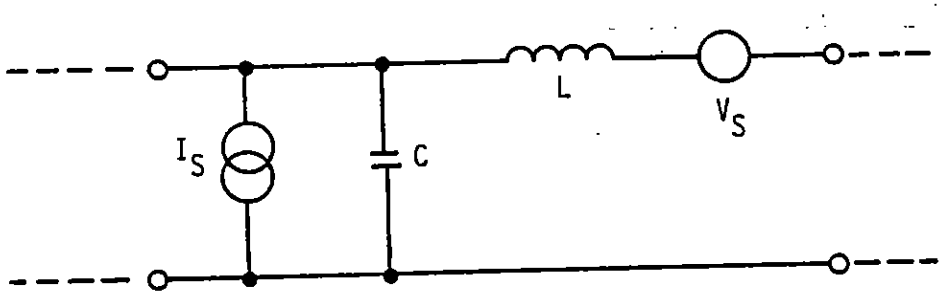

Figure 19. Excitation sources per unit length in a transmission-line segment

shown in Figure 18, using a two-dimensional particle-pusher code in conjunction with a finite-difference (Refs. 1,2), Green's function (Ref. 13), or lumped-element (Refs. 3,14) approach. The current emitted from the ground plane, the current passing through the imaginary surface, and the potential of the arbitrary surface and ground plane comprise a sufficient specification of the boundary condition to solve the problem.

A numerical solution is obtained for the open-circuit voltage as a function of time for the isolated conducting rod. Contributions to the open-circuit voltage come from:

1. changing potentials on the boundary,
2. charge in the volume,
3. charge striking the conducting wire.

The equivalent circuit current generator is simply

$$I_S = C \dot{V}_{OC} , \qquad (4\text{-}1)$$

where C is the capacity of a rod over a ground plane.

4.1.2 Solution Technique 2

This technique is essentially the same as the one described above, with the additional simplifying assumption that the potential changes slowly in a direction perpendicular to the wire and parallel to the conducting plane. The arbitrary surface in the vicinity of the cable can be formed by an equipotential surface or conducting plane, as shown in Figure 20. This assumption permits a rather simple geometry in which the arbitrary surface above the ground plane is assigned a time-dependent potential

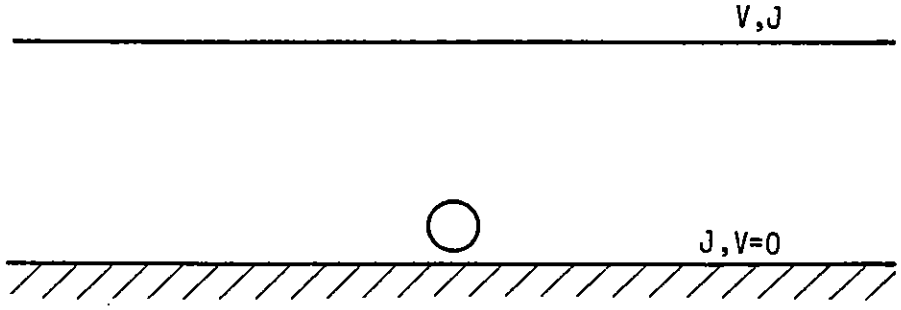

Figure 20. Cable configuration with arbitrary surface formed by an equipotential (conducting) plane

equal to that existing at an equivalent point in space in the unperturbed structure (in the absence of the cable). The resulting problem can be readily solved by using existing techniques such as the quasi-static PC code (Ref. 15).

4.1.3 Solution Technique 3

This technique utilizes the simplifying assumption that the potential is unperturbed by the presence of the cable. The source terms are computed directly from (1) the potential V_C at the point where the cable lays, and (2) the net current striking the cable:

$$I_S = C \dot{V}_C + \int (\vec{J}_{IN} - \vec{J}_{OUT}) \, d\vec{S} = C \dot{V}_C + \frac{dQ}{dt} . \qquad (4\text{-}2)$$

The quantity $J_{IN} - J_{OUT}$ is the net current striking the cable, Q is the net charge striking the cable, and $d\vec{S}$ is an element of cable surface area.

A problem arises in defining the potential V_C for cables very near the ground plane when the height-to-diameter ratio, h/d, is small. Computational techniques have been developed to define the effective height at which the potential should be computed (Ref. 16).

Of the three techniques described, the first is the most accurate, but it is also the most time-consuming. We speculate that the third technique should be nearly as accurate as the first two in the linear regime, where the electron trajectories are not altered by the presence of the cable. In this low-level regime, the only significant perturbation introduced by the cable is that the cable displaces a certain amount of charge which otherwise would have been present to produce a changing electric field. This effect may be significant only when the cable is near the ground plane, and can be addressed simply by incorporating the perturbation in the effective height computation.

4.2 NONLINEAR SOLUTION FOR A SINGLE CABLE

At higher emission current levels, the problem becomes nonlinear because the potentials in the space surrounding the structure are on the same order of magnitude as the emitted electron energies. Thus, a region of high electron density forms near emitting surfaces. The presence of

a cable in the space-charge barrier can severely perturb the local electron dynamics, the local electric fields, and the currents striking the cable.

The solution technique for this problem is essentially the same as described in the previous section except that the technique must be self-consistent to account for space-charge-limiting. The fundamental difference between the linear and nonlinear problems, insofar as forming the transmission-line model source is concerned, is that the electron motion at each cable segment depends upon the local potential which, in turn, depends upon the remainder of the cable and the cable load characteristics. Thus, the two-dimensional solutions for each segment are coupled through the cable potential. Several approximate solution techniques for treating this problem are described below.

4.2.1 Solution Technique 1

The most obvious way to treat this problem is to solve each two-dimensional segment simultaneously with the transmission-line solution so that the instantaneous potential of each cable segment is known. At each time step, the electron dynamics are solved with the cable held at the potential computed by the transmission-line model. Charge motion is advanced during the time step and the open-circuit cable voltage is then computed. The current generator for each segment is computed as before:

$$I_S = C \dot{V}_{OC} .$$

It is important to realize that there are two potentials which must be considered at each time step. One is the actual cable potential V at a given segment, which controls the electron dynamics. The other is the open-circuit voltage V_{OC} induced on an unloaded cable segment as a result of the charge motion, which is used in forming the excitation current generator. In general, $V < V_{OC}$ unless the cable is unloaded, in which case the two are equal.

4.2.2 Solution Technique 2

The previous technique requires a considerable amount of computation which can be avoided in many cases. With several additional assumptions, the computations can be significantly simplified:

1. The electron transit time between the emitting plane and the space-charge barrier region is small relative to the times of interest in the emission current pulse.
2. The electrons entering the volume through the imaginary surface are unperturbed by the cable potential.

The first assumption is equivalent to assuming that the space-charge barrier sets up quickly and becomes essentially quasi-steady through most of the problem. Typical space-charge barriers peak at 5 to 10 cm from the emission surface, while typical transit times for electrons reaching the vicinity of the barrier are

$$t \approx \frac{d}{v} \approx \frac{0.1}{0.1c} \approx 3 \text{ nsec} .$$

The time is short compared to most pulse widths of interest. For shorter pulses, the barrier sets up considerably sooner than 3 nsec.

The second assumption is also generally valid because the electrons entering the volume through the arbitrary surface must have escaped a space-charge barrier at some other surface and, therefore, must consist of relatively high-energy electrons. These high-energy electrons are, to the first order, unperturbed by the presence of the cable.

With these two assumptions, the charge motion need not be computed using the updated potential determined at each time step by solving the transmission-line problem simultaneously. Rather, the solution is repeated several times, each time computing the electron dynamics with a fixed potential, V. In this way, a matrix of current sources is computed, the instantaneous value of each depending upon the cable potential as well as on the time:

$$I_S = C \dot{V}_{OC} (V_{cable}, t) .$$

4.3 SINGLE CABLE SURROUNDED BY A DIELECTRIC INSULATOR

Consider next a single conductor surrounded by an insulating dielectric laying above a ground plane. The treatment of magnetic and electric

fields from the structure is similar to that discussed in the previous section and will not be repeated here. However, the treatment of excitation sources arising from currents striking the cable become more complex because of the dielectric. In the remainder of this section, we ignore the magnetic and electric field sources and concentrate on those arising from charge deposition in the dielectric.

As in the case of the coaxial cable, excitation occurs because of charge accumulation at both the conductor-dielectric interface and the vacuum-dielectric interface, as well as in the dielectric bulk. For cables located a distance from the ground plane that are large relative to the thickness of the dielectric, the distribution of these charges in the dielectric is unimportant, and the cable excitation depends only upon the total charge accumulating. This situation is virtually identical to the single conducting cable without a dielectric insulator. However, for cables whose distance from the ground plane is comparable to the insulation thickness, the distribution of the charges in the dielectric is important in determining net current flow in the cable.

It should be recognized that the worst-case cable response can be estimated by assuming that all the charge striking the dielectric actually strikes the conductor. The details of the charge distribution need not be considered, and the solution technique of Section 4.2 applies. In practice, the approximation should be very good because only a small fraction of the wire insulator is near the ground plane, even when the cable is laying directly on the ground plane. Nevertheless, this configuration is worth pursuing in more detail if only as a prelude to the discussion of multiple-wire bundles.

4.3.1 Solution Technique 1

The solution to the problem can be obtained using the same technique described in Section 4.1.1 for a single non-insulated wire. The Poisson equation is solved for the charge distribution obtained from electron transport calculations to obtain the open-circuit voltage V_{OC} on the cable. The current source for the lumped-element model is given by Eq. 4-1, as before. There is no basic difference between the treatment of insulated and uninsulated wires using this approach.

4.3.2 Approximate Solution Technique

The goal here is to formulate a simple approximate technique which can be repeatedly employed in system studies without the need to solve Poisson's equation each time. In formulating such a simple approximate technique, we are confronted with the problem that the current source, $I = dQ/dt$, cannot explicitly be represented by a connection directly between the ground plane and the cable, since the charge does not reach the conductor but, rather, is stopped somewhere in the dielectric. It would be most convenient to form a model in which the source dQ/dt appears explicitly, such as the one shown in Figure 21a. Unfortunately, the approach shown in the figure will work only if the ring of charge lays on an equal potential. Due to the lack of symmetry, charge located at a radius r does not in general lay on an equal potential line formed by a circle passing through the point r concentric with the wire.

One viable approach is to break up the charge into a number of segments, as shown in Figure 22a, each of which may have a different potential with respect to the conductor. The equivalent circuit for the configuration is shown in Figure 22b. The problem of computing each of the partial capacities is significantly more complex than for the coaxial cable because of the lack of symmetry. A rigorous approach for computing partial capacities is discussed in the section on multiple-conductor systems.

An alternate approach is to develop appropriate approximate techniques to adequately define the partial capacities. Appropriate approximations might include:

1. Neglecting intercapacity terms C_{ij}.
2. Dividing the capacitors C_{Ai} equally such that $\sum C_{Ai} = C_A$, and choosing C_{Bi} such that $\sum (C_{Bi}\ C_{Ai})/(C_{Bi} + C_{Ai}) = C$ where C is the total capacity of the wire to ground.

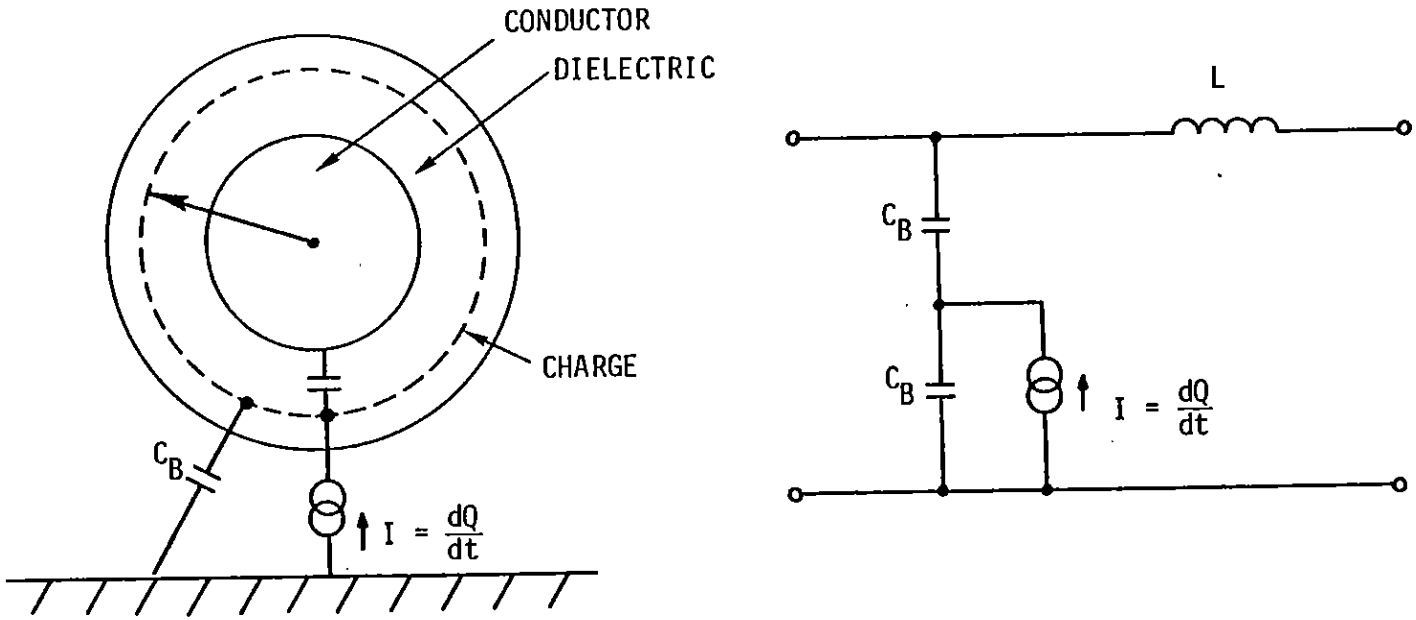

(a) Schematic of wire and dielectric

(b) Equivalent circuit

RT-11484

Figure 21. Model formed by assuming the ring of charge at radius r lies on an equipotential surface

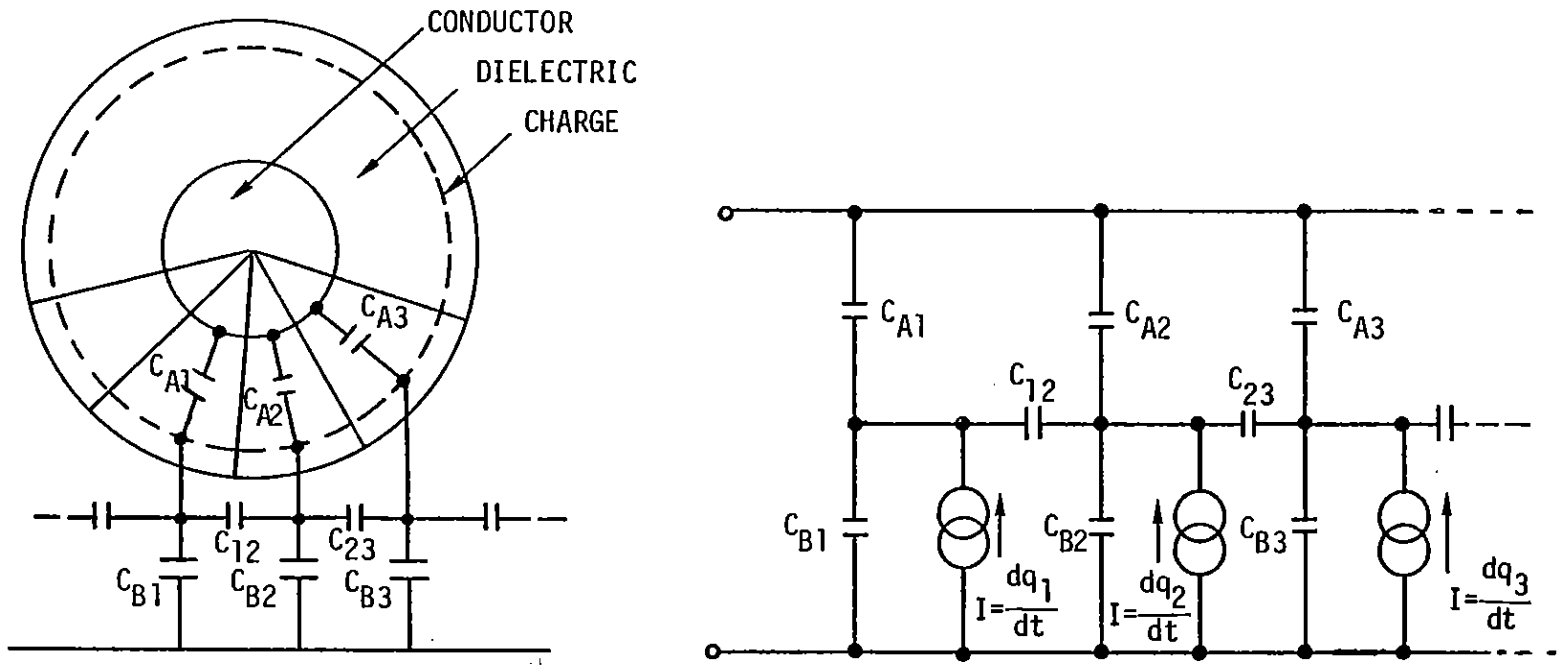

(a) Schematic of wire and dielectric

(b) Equivalent circuit

RT-11483

Figure 22. Model formed for a wire surrounded by a dielectric using the method of partial capacities

5. MULTIPLE CABLES

In the previous sections, we have discussed single-wire configurations which can be treated quite rigorously by simply solving Poisson's equation for the open-circuit voltage on the single wire. In principle, this technique can be extended to multiple-wire configurations. In practice, the concept of performing an electron transport and Poisson's equation solution on anything more than several wires becomes quite impractical. If a solution for more than several cables is desired, it will be absolutely necessary to form approximate models.

To validate appropriate approximate models, it is useful to investigate two- or three-wire bundles to (1) determine the importance of each excitation source, (2) verify the accuracy of the approximate solution technique, and (3) quantify the uncertainty associated with the approximations. A rigorous approach to computing the lumped-element model current sources is considered first, and then suggestions are made for more approximate models.

For unshielded cables, electron trajectory perturbations (where required, such as for space-charge-limited computations) can be found by treating the cable as a single wire and employing the techniques described in previous sections. The results of these calculations will define the spatial distribution of electrons striking the bundle. This information can then be used in forming the lumped-element model. For shielded cables, nonlinear electron transport need not be considered.

In all cases, we begin by assuming that appropriate electron transport and deposition calculations have been performed. We also assume that the unperturbed electric and magnetic fields from the surrounding structure have been determined for use in computing unshielded cable excitation. The computation of multiple-wire excitation by electric and magnetic fields is identical to the treatment for EMP excitation and is not considered here. The fundamental problem we address here is the excitation source arising

from net charge accumulation in the dielectrics surrounding the individual cables in the bundle.

The sources of excitation arise from charge accumulation due to:

1. Photon attenuation in the dielectric bulk.
2. Imbalance in emission efficiency at the dielectric-core interface.
3. Net charge transfer between cable dielectric surfaces.
4. Net charge transfer between individual wires and the reference plane.

5.1 RIGOROUS APPROACH

The most rigorous approach consists of computing the open-circuit voltage on the individual wires by solving the Poisson's equation for the multiple-wire system. A three-wire system is shown in Figure 23, while the equivalent circuit per unit length for such a system is shown in Figure 24. The technique for computing the partical capacities C_{ij} is identical to the technique used in cable computation for EMP excitation. A brief discussion of the approach is given in Reference 17. Capacitors C_1, C_2, and C_3 appearing in the current sources represent the total capacity of wires 1, 2, and 3, respectively, to the reference plane (either the ground plane or the cable shield).

Note that no current sources are required between the various conductors. The open-circuit voltage on each cable is correctly computed from each individual current generator which contains information on the presence of other cables through both the capacity C_i and the open-circuit voltage V_{OC_i}. Mutual inductances may be computed as necessary but are not specifically shown.

5.2 APPROXIMATE TECHNIQUE

In principle, this approach can be executed quite easily. In practice, a number of approximations are required. The most obvious approximation is to replace the charge distribution in the dielectric by several layers of charge located at effective radii so that the cable excitation is effectively equal to that produced by the entire spatial distribution.

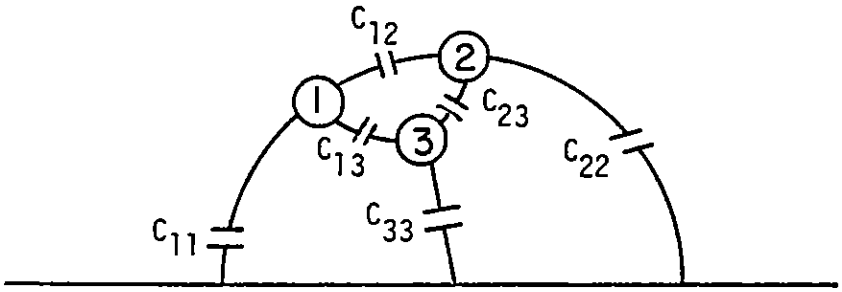

Figure 23. Multiple-wire configuration

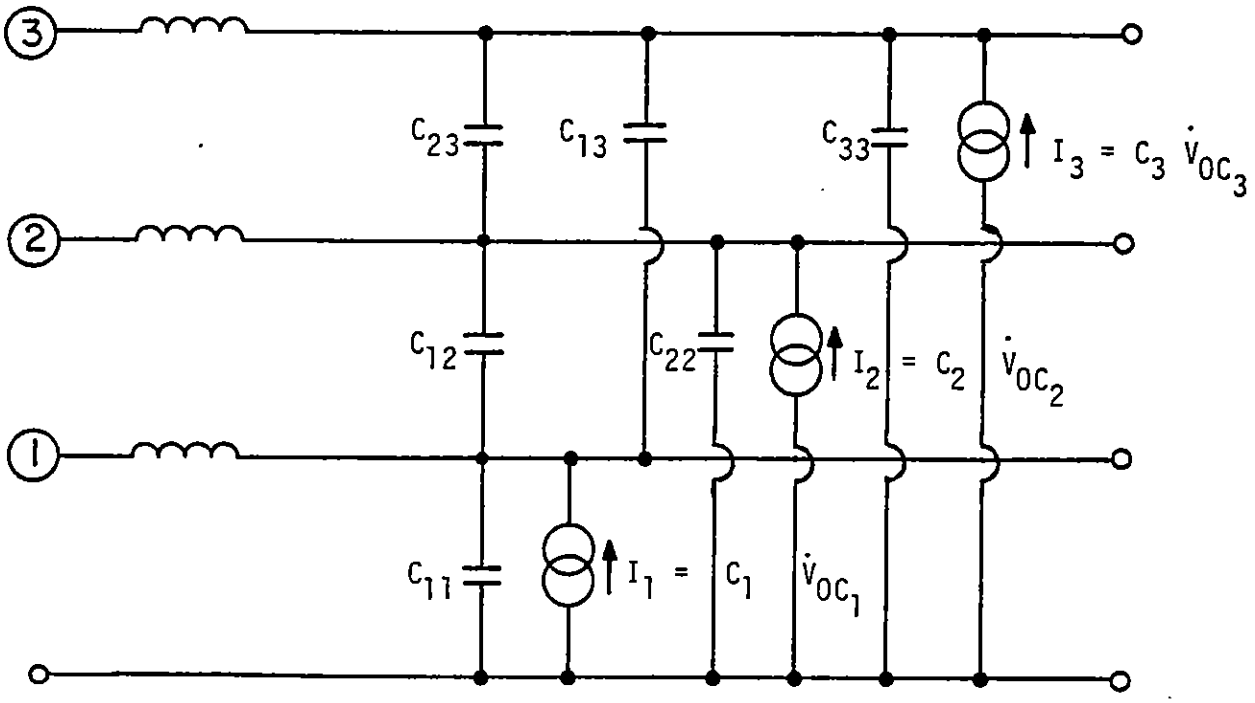

Figure 24. Equivalent circuit for three-wire configuration shown in Figure 23.

Equivalent charge layers are required for each of the four sources of excitation listed on page 39. A solution technique using lumped-element circuits, Green's function, etc., can be used to solve the Poisson's equation for the resulting open-circuit voltage.

One disadvantage of this approach is that the numerical difficulties increase with the increasing numbers of wires. Furthermore, the current sources, expressed in terms of time derivatives of open-circuit voltage, are not easily related to the real current dQ/dt which forms the driving function for the excitation. Therefore, it is desirable to reformulate the problem so that the real current sources are explicitly represented. We shall see that to accomplish this practically, several approximations are required.

Consider a two-wire cable surrounded by a shield, as shown in Figure 25. Charge accumulation at the core-dielectric interface and charge accumulation from the shield-dielectric interface are shown. For purposes of this discussion, sources arising from charge transfer between wires and from charge accumulation in dielectric bulk due to photon attenuation are not considered. One might be tempted to define partial capacities between each of the conductors and segments of charge, as shown in Figure 25. Such an approach will work only if the charge is located on equipotential contours, a condition which is not met in general (except for the coaxial cable). This simplistic approach leads to the model shown in Figure 26 and is used by Wilson and Trybus (Ref. 9) in an approximate treatment of a seven-wire bundle. The results of such a model are questionable because of the equipotential assumption required.

An alternate approximate approach, consisting of dividing the charge rings up into a number of angular bins so that each segment can assume a different potential. The problem here is that the number of partial capacitors can rapidly increase as the segment size is reduced. If we set the number of segments equal to the number of cables in the bundle and ignore partial capacities between the adjacent charge segments, we arrive at a potentially valid model which is also tractable. Such a model is shown for the two-wire system in Figure 27. Capacitors C_2,

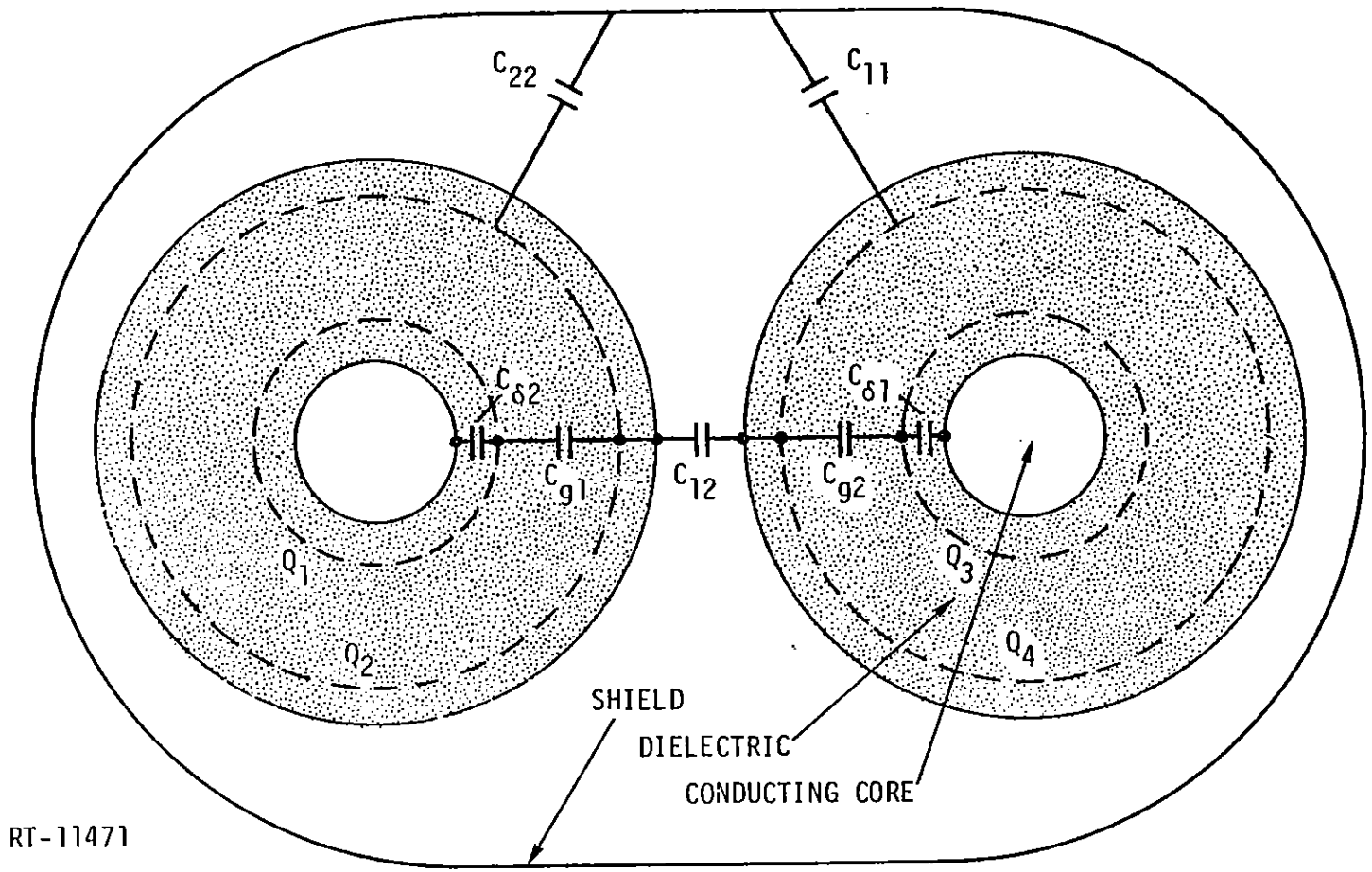

Figure 25. Schematic of two-wire cable within a shield. Capacitors are connected between charge rings, which are assumed to be located on equipotential contours.

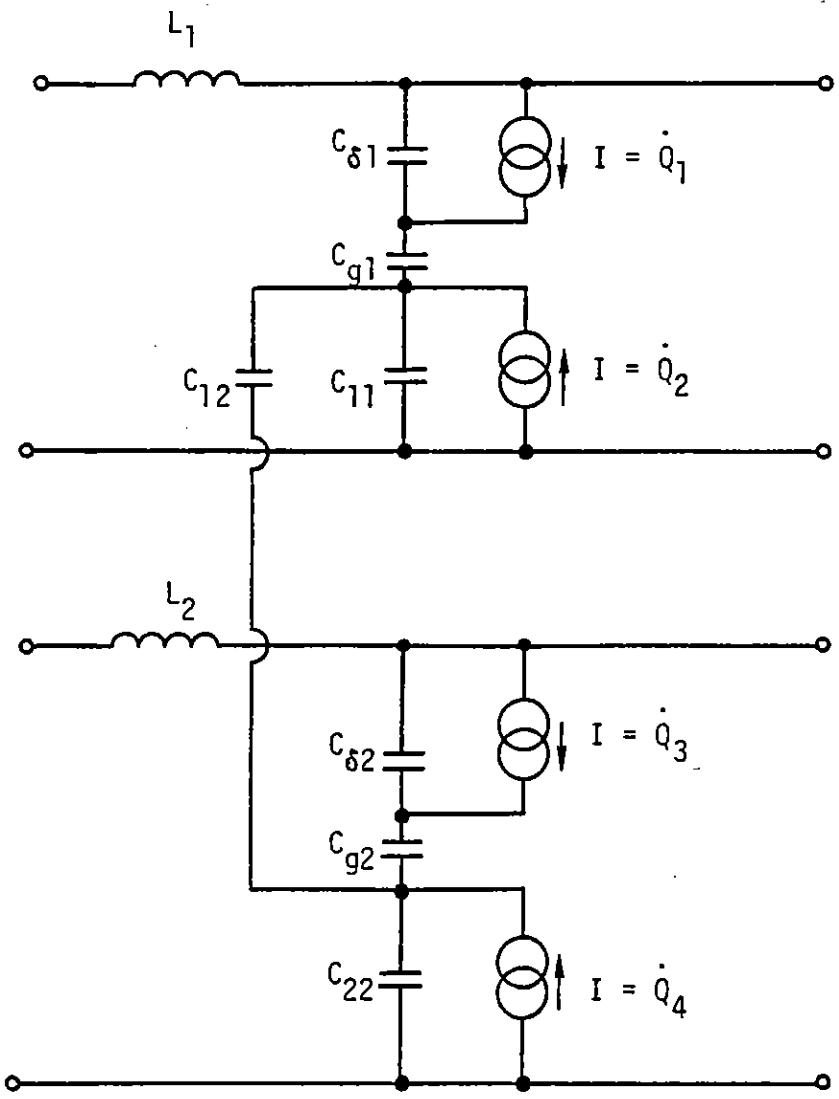

Figure 26. Equivalent circuit for a two-wire bundle within a shield, assuming that the charge lays on an equipotential surface

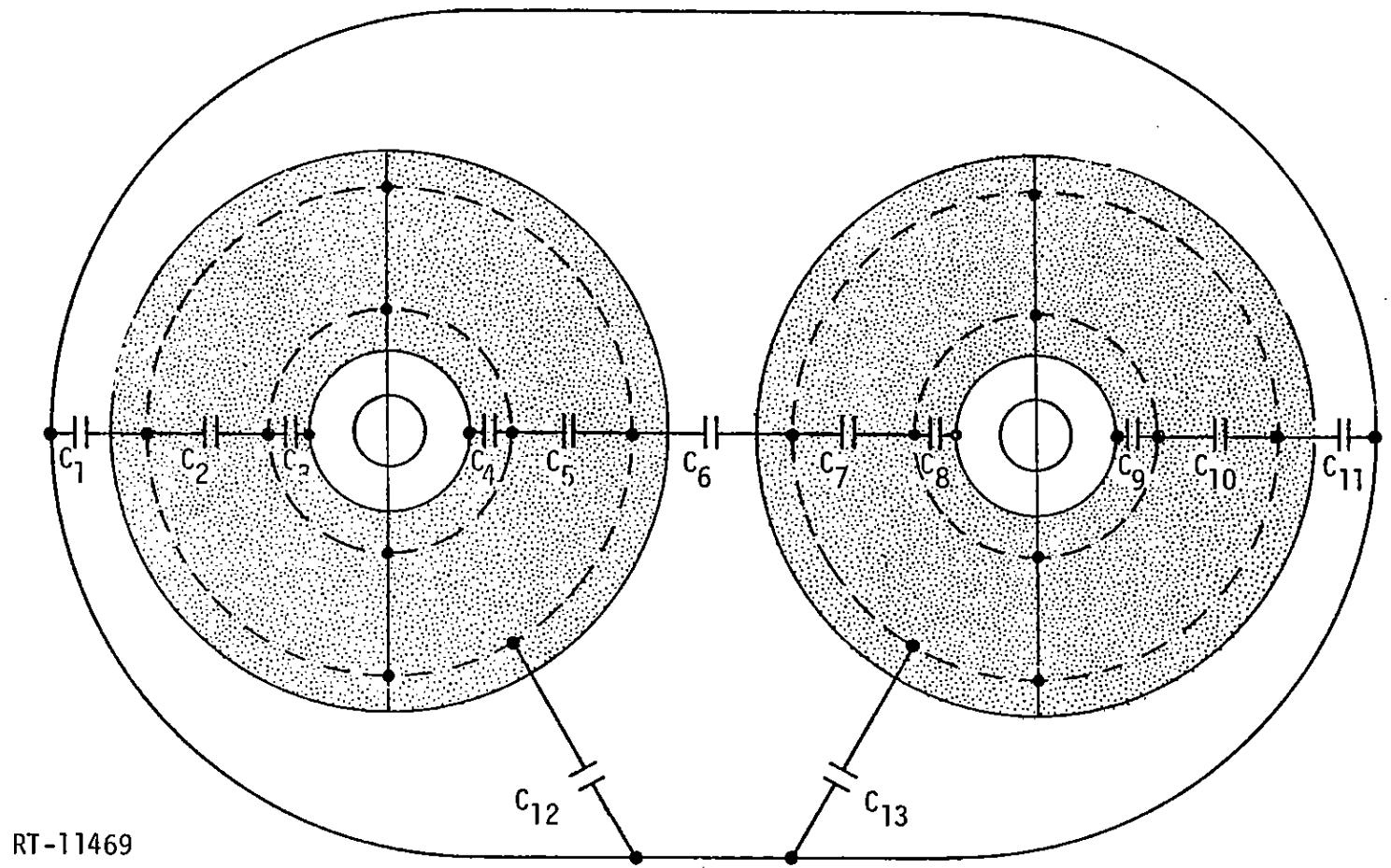

Figure 27. Two-wire system for which the charge rings are broken into a number of segments equal to the number of cables. Partial capacities between segments are assumed to be small.

C_3, C_4, C_5, C_7, C_8, C_9, and C_{10} can be computed by assuming them to be half the capacity between appropriate concentric conductors; C_6 is the partial capacity between two conductors located at a radius where the outer charge layer resides; and the parallel combination of C_1 and C_{12} is the partial capacity C_{11} of a wire to the shield. As a first approximation, $C_1 = C_{11}$ and $C_{12} = 0$. The lumped-element model for one wire of the bundle is shown in Figure 28.

Source terms for charge transfer between wires and for buildup in the dielectric bulk can be readily incorporated into this model. Of course, the validity of such a model is still in question but it can be verified by comparing with the more exact solution techniques described in Section 5.1.

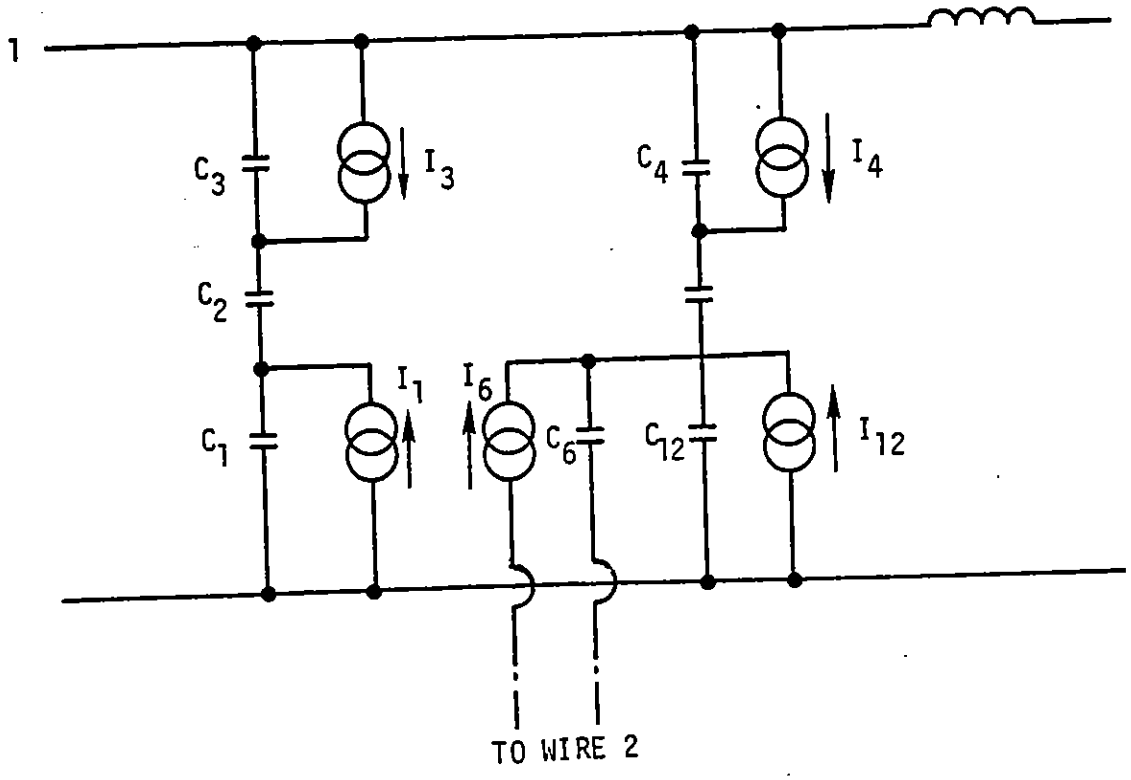

Figure 28. Equivalent circuit for one wire shown in Figure 27

6. SUMMARY AND CONCLUSIONS

6.1 STUDY OBJECTIVES

The computation of currents leading into electronics boxes, is a necessary step in the SGEMP assessment process. Despite the difficulties that have plagued cable computations in the past, this step is every bit as important as SGEMP structural calculations and must be considered at some point in the SGEMP assessment of systems.

We feel that the objectives of an investigation of the cable response in an SGEMP environment should be to:

1. Understand the excitation mechanisms involved.
2. Determine how the response changes with changing fluence, x-ray energy, load impedance, number of cables, etc.
3. Provide a reasonable bound on bulk and/or individual wire currents.
4. Provide simple approximate computational techniques for use in system studies.
5. Validate the computational techniques by comparison to experimental data.

6.2 SUMMARY

A brief summary of the efforts described in this document follows.

1. Problem Methodology

   A methodology for addressing the cable problem has been defined, beginning with the complete three-dimensional problem of the cable coupled to the structural response and continuing through to two-dimensional transmission-line models, including:

- 3-D solution for cables coupled to structures,
- approximate techniques for decoupling the cables,
- 3-D solution techniques for decoupled cables,
- Transmission-line models with 2-D excitation sources.

2. Definition of Excitation Sources

Lumped-element models have been identified for each of the pertinent excitation source terms, including:

- unperturbed electric and magnetic fields generated by the portion of the structure away from the vicinity of the cable,
- locally perturbed electric fields in the vicinity of the cable,
- charge deposited onto conducting cables,
- charge deposited onto dielectrics surrounding cables.

3. Cable Configurations

Three basic types of cables were considered in varying degrees of detail:

- shielded single coax,
- single wire over a ground plane,
- multiple wires.

6.3 PERTINENT RESULTS

We consider the following results to be pertinent.

1. A technique has been defined whereby the excitation from unperturbed electric and magnetic fields generated in the structure away from the cable region can be smoothly meshed to the decoupled solution of the locally perturbed currents and fields in the vicinity of the cables.
2. The quasi-static solution technique for currents and fields in the plane transverse to the cable is shown to be valid and consistent for use with the transmission-line model. Conversely, the conditions for which the quasi-static model is not valid for computing the transmission-line source terms are also the conditions for which the transmission-line model is invalid.

3. Charge accumulation in the bulk of the dielectric arising from photon attenuation is equally as important a source of excitation in shielded cables as is charge accumulation at dielectric-conductor interfaces due to unequal emission efficiencies.
4. In general, rings of charge deposited in a dielectric insulation equidistant from the core of a wire do not lay on an equipotential surface (except for the single case of a coaxial cable). Thus, approximate techniques whereby capacitors are used to interconnect various rings of charge to conductors as if the rings were on equipotential surfaces are suspect.

6.4 RECOMMENDATIONS

We make the following recommendations for future work.

1. Complete the rigorous approach for computing the two-dimensional excitation source terms begun under the Analysis Verification effort (Ref. 9).
2. Validate the transmission-line model for several configurations of interest to the satellite problem, using the 3-D SGEMP codes such as the Maxwell's equation equivalent circuit (MEEC) approach.
3. Exercise the transmission-line models to identify important sources of excitation.
4. Compare predictions with experimental data.
5. Define approximate methods of computing important excitation source terms useful for systems work. Validate these models by comparing with the more exact two-dimensional treatment.
6. Document results.

APPENDIX A

DEVELOPMENT OF SGEMP CABLE CODE

1. INTRODUCTION

The purpose of this appendix is to summarize the status of the bulk cable code development under TD 01-05 of contract F29601-74-C-0039. Although work on this project has been performed by both Intelcom Rad Tech (IRT) and Mission Research Corporation (MRC), this appendix covers only the work by IRT. In Section 2 the objectives of this program are restated, and Section 3 describes various approaches that were taken and their degrees of success. The present status of the code development is given in Section 4. MRC calculations appear in Volume 2.

2. OBJECTIVES

The overall objective of this program is to develop a computer code (or codes) that can predict the response of a cable or a bundle of cables to a pulse of radiation. The cables of interest at present are coaxial cables and bundles of insulated unshielded cylindrical wires at various distances from a conducting ground plane or with a conducting sheath around the cable bundle. The perturbing effect of the radiation pulse is due both to photon-induced charge distributions in the dielectrics of the cables and to the capture of secondary electrons from the walls of the cavity by the dielectric insulation around unshielded cables.

The major steps which should be included in the code are the following.

1. Energy and angular distribution of secondary electrons which come from the cavity walls and impinge onto the outside of the cables.
2. Photon attenuation through the cables.
3. Electron transport in the cables (that is, electron emission from metal to dielectric and from dielectric to metal) and electron transport in the bulk of the dielectric.

4. Charge deposition profiles in cable insulations and net charges on the cable conductors and cavity walls due to items 1 and 3.
5. Calculation of relative potentials between the different cables and the cavity wall (ground plane) due to the charges from item 4 and conversion of these potentials to current generators for small longitudinal segments of the cable.
6. Response of the cable to the current generators from item 5 including transmission-line effects.

Some of the above items are already available from other codes, and it is mainly a matter of incorporating them into a single code for the cable response, as discussed in Section 4. However, the calculation of the potentials (item 5) can be complicated, even for such a relatively simple geometry as two parallel insulated unshielded cables, and it becomes even more complex when a ground plane, a wraparound sheath, or additional wires are added. Thus, a major portion of the effort by IRT so far has been devoted to this item.

3. APPROACHES THAT HAVE BEEN USED TO OBTAIN POTENTIAL DIFFERENCES

Most of the work by IRT thus far has been to determine the potentials on the different wires for various distributions of charge trapped in the dielectrics of the cables. Five main approaches have been tried, with differing degrees of rigor and success. In their order of time sequence, these were (a) the use of a few capacitors to estimate the coupling between wires, (b) a finite-element solution of Poisson's equation for the potentials on cables and walls due to arbitrary charge distributions, (c) multiple images, (d) an exact solution for coaxial wires, and (e) a partial-capacitance method for approximating the solution of Poisson's equation. Each of these approaches is discussed below. The main reason for describing the methods which were not successful is to point out some pitfalls that are not always obvious without some investigation and hopefully to prevent some useless duplication of work by other investigators.

3.1 COUPLING BY A FEW CAPACITORS

The first approach that was used in an attempt to find the potentials between insulated unshielded cables over a conducting ground plane was to couple the conductors together by their capacitances to each other and by psuedo-capacitances to the trapped charge. As a specific example, a single insulated wire over a ground plane was considered with a uniform ring of trapped charge in the dielectric around the cable. It was then intended to replace the ground plane by the image of the cable and its fixed charge. The capacitances between each conductor and its ring of charge and between the cable and its image would then be used to determine the potential differences due to the trapped charge.

There are two major difficulties with this procedure. First, as discussed later in Section 3.3, it is not possible to rigorously replace a cylindrical conductor and its insulating coating with a finite set of images. A rough approximation might be made with various assumptions, but one would always wonder about the sensitivity of the results to those assumptions.

The second difficulty is that capacitances have meaning only between equipotential surfaces. The charges in these surfaces are free to move around to cause the surfaces to remain equipotentials. For example, when a charged cylinder is brought close to a ground plane, the excess charge in the cylinder is attracted by the compensating charge in the ground plane and the excess charge in the cylinder tends to accumulate on the portion of the cylinder closest to the plane. By contrast, the charge that is assumed to be trapped in a ring around the conductor is not free to move, and the ring will not, in general, be an equipotential surface. Therefore, this method is not correct and has been abandoned.

Since essentially this same procedure of taking capacitances to trapped charge is fairly common in the industry, one should be aware of the basic assumptions and limitations. Although it is not strictly correct to use a capacitance to a region of trapped fixed charge, the approach is not too inaccurate if the regions of trapped charge are not too large and the potential over the region is approximately constant. If the ring of charge around the cable in the previous

example is broken up into a number of adjacent capacitors so that each small arc of the ring is more nearly an equipotential surface, then the method becomes more accurate. In fact, this is the basis for the partial-capacitance method discussed later in Section 3.5. In that method, all of the space between the conductors is divided up into a mesh of nodes and connecting leads. The capacitances between adjacent nodes are chosen essentially assuming that a small fictitious surface through each node perpendicular to the line to the next node is a conducting surface. Thus, all of the space is divided into small conducting surfaces which then react with their nearest neighbors through their respective capacitances. This method becomes increasingly rigorous as the mesh sizes are made smaller. Conversely, the accuracy decreases if the imaginary equipotential areas become large compared to the other important dimensions in the problem.

3.2 FINITE-ELEMENT SOLUTION OF POISSON'S EQUATION

The solution of Poisson's equation with appropriate boundary conditions is, of course, the most rigorous and complete method for determining the potentials between the conductors. Unfortunately, closed-form solutions are usually possible only for relatively simple cable geometries and symmetric charge distributions. For more complicated situations, computer codes are often used to solve the equations in finite-difference or finite-element form. In the finite-difference technique, the space of interest is divided into a spatial mesh and the partial differential equations are approximated by finite-difference derivatives. The resulting algebraic equations are then solved either by matrix inversion or by some iterative procedure. In the finite-element approach, the space of interest is again divided into a convenient mesh. The integral of a potential energy function over the mesh area is then minimized to find the correct potentials for the given charge distribution.

In principle, both of these methods can be made as accurate as desired by making the spatial mesh grids sufficiently small. However, there is always the inaccuracy of approximating curved surfaces with straight line

grids. Also, from practical considerations, there are limitations on the number of mesh regions due to computer storage, computation time, and roundoff errors. In spite of these limitations, these methods can be powerful tools, especially for providing a few good check runs with which simpler calculations can be compared.

Since a finite-element computer code was available, this method was applied to a single insulated unshielded wire over a conducting ground plane for a symmetric ring of trapped charge in the insulation around the wire. This code could handle a more realistic distribution of trapped charge with no additional complication to the method. However, in the absence of a specific realistic distribution of interest, this simple uniform ring distribution was used.

This code was originally written to find the potential difference between conductors for a given distribution of charge. However, to obtain current generators for use in transmission-line codes, the amount of charge that would flow between the wire and the wall to equalize the voltages caused by the trapped charge was required. Therefore, the code was run with the cable conductor and wall shorted together (zero potential difference). The charges on the wire and the wall were then calculated by integrating the derivative of the potential normal to the conductor surfaces (which is proportional to the local surface charge density) over the respective areas of the conductors. By charge conservation, the algebraic sum of the charge in the wire and the wall should equal the charge trapped in the insulator. In early attempts with this method, the inaccuracies in taking normal derivatives over finite distances and in approximating the curved surface of the wire by straight line segments caused by a discrepancy in the integrated surface charges on the order of 25% of the trapped charge. However, later refinements of the mesh reduced this error to less than ±10%, which is adequate for most practical estimates of the current generators.

Although the above results are reasonable for a single wire over a ground plane, the addition of other wires would require setting up a new mesh grid, which involves a significant amount of manual labor, an

increase in computer costs from the previous $5 to $10 per run, and probably some readjustment of the initial mesh selection to give acceptable accuracy in the integrated charge. Thus, although the method can give good answers, it is not convenient for complex cable arrangements. Therefore, an alternative method was sought which would be reasonably accurate and more user-oriented. This search next involved using multiple images, which is described in Section 3.3 and which was not successful for a dielectric of finite thickness over a cylindrical conductor, and the method of partial capacitances, described in Section 3.5, which led to the exact solution for coaxial cables described in Section 3.4.

3.3 MULTIPLE IMAGES

The method of images is a very powerful tool for finding the electric fields and potentials due to discrete line charges near conducting cylinders or ground planes. For a single line charge parallel to a conducting ground plane or a bare conducting cylinder, the conducting surfaces can be replaced by a single image line charge across the conducting surface from the real line charge. For more than one bare conducting surface, the image system for a single real line charge is an infinite series of images. The infinite series arises from imaging the real charge in each conductor and then imaging those images into the other conductors, etc. Fortunately, this series converges rapidly, and with computer programs, it is quite practical to obtain very accurate values for the potential differences. The main problem is the bookkeeping to keep track of which charges or images have been imaged across which surfaces. This method has been used extensively to obtain a few "exact" solutions for checking the partial-capacitance results in Section 3.5.

Thus far, this discussion has been confined to bare conductors. In most practical configurations, the cable conductors will be covered with a finite thickness of insulation. Charges can be trapped inside and exterior to this insulation — for example, in other cables. Thus, to use the multiple-image method, one needs the image solution for a line charge near a cylindrical conductor surrounded by a finite-thickness insulator.

In Classical Electricity and Magnetism* (p. 66), it is shown that a real-line charge can be replaced by a relatively simple set of images, whose strengths are functions of the dielectric constant of the cylinder. In an attempt to find an equivalent solution for a conducting cylinder surrounded by a finite thickness of insulation, this procedure was repeated for this geometry. It was a straightforward process to obtain the solution to the problem in general form. Unfortunately, the terms in some of the resulting infinite series had some extraneous multiplying factors, so it was not possible to interpret the resulting series in terms of a finite set of images. This is one of the reasons why the initial attempts to calculate the coupling between cables and a ground plane (Section 3.1) were unsuccessful. Therefore, this method had to be discarded except, as mentioned above, for obtaining a few check solutions using bare conductors, in which case the method is valid and accurate.

3.4 EXACT SOLUTION FOR COAXIAL CABLE

When the partial-capacitance method, which is described later in Section 3.5 of Appendix A, was applied to a single line charge q between two concentric conducting cylinders, it was found that the potential difference between the two cylinders was the same as if the charge q were uniformly distributed in a thin cylindrical shell at the same radial position as the line charge q. The local electric fields for the single line charge were not the same as for the cylindrical shell of charge; only the potential difference between the two cylinders was the same. Subsequent analyses using images and the solution of Laplace's equation by the method of harmonics has shown that this is an exact result for coaxial cables, not only when the space between the conductors is a uniform dielectric but also when there are cylindrically symmetric gaps. The proof for a uniform dielectric using the method of images is given in Appendix B, but for brevity, the more general result for gaps in the dielectric using the solution of Laplace's equation is not given in this report.

*W. K. H. Panofsky and M. Phillips, Addison-Wesley Publishing Co., Reading, Mass. (1956).

This result has some interesting and useful consequences. First, when one is interested only in the potential difference between the conductors (and not in the local electric fields in the dielectric), it is not necessary to solve the problem for the actual distribution of charge, which usually is non-uniform in both the radial and azimuthal directions. The above result says that only the radial distribution of charge in the dielectric (and the net charge in the two conductors) has an effect on the potential difference between the conductors. Thus, if the non-uniform distribution of charge throughout the dielectric and the compensating charges in the two conductors are known, the potential difference between the two conductors can be found by averaging the charge distribution at each radius over the complete azimuthal angle and then integrating the radial portion of Poisson's equation in cylindrical coordinates between the two conductors. This is the procedure that will be used for the coaxial cable code, as discussed later in Section 4.1.

The second interesting consequence of this result is that models which approximate the radiation effects in a coaxial cable by radial capacitances (1) from the center conductor to the trapped charge and (2) from the trapped charge to the outer conductor will give the exactly correct potential difference between the cable and its sheath, regardless whether several or only one radial capacitor is used to represent the interaction between the center conductor and the ring of charge and between the ring of charge and the outer conductor. The only requirement for obtaining the exact result is that the correct radial capacitances be used. If only one capacitance is used between a conductor and the ring of charge, its value must obviously be the capacitance between two concentric cylinders with the same radii. If more than one capacitance is used, their sum must equal the value for a single capacitor.

A word of caution is in order regarding this discussion. Averaging the charge around the circumference and using only one radial capacitance out to the trapped charge and another to the outer conductor gives the correct potential difference only for a coaxial cable. For unshielded insulated wires, with or without ground planes or wraparound shields, a more complete set of partial capacitances is needed, such as described in Section 3.5 of Appendix A.

3.5 PARTIAL-CAPACITANCE METHOD

The partial-capacitance method is essentially also just a solution of Poisson's equation except that it uses a mesh of capacitances with charge distributions at the nodes of the mesh instead of a finite-element solution of the equations, as in Section 3.2. In this method, the region between the cable conductors (and the ground plane, if present) is divided into a convenient spatial mesh, similar to a finite-difference or finite-element grid. The intersections of the grid lines are nodes and the adjacent nodes are connected by capacitances. The solution of the circuit equations for arbitrary charge distributions on the nodes and on the conductors yields the voltages between all nodes and, therefore, between all conductors. These voltages can then be converted to current generators corresponding to the radiation pulse that caused the initial charge distribution.

The accuracy of this method depends on the selection of the grid and the estimation of the capacitances between the nodes. Since the present cables of interest have circular cross sections, it is convenient, and probably most accurate, to choose a grid system using concentric circles about a cable and radial lines from its centerline. However, for more than one wire and/or with a ground plane, the pattern of concentric circles and radial lines and the corresponding capacitances must be modified at the line of symmetry between the wires and at the ground plane. A typical grid for two parallel wires is illustrated in Figure A-1. The correctness of the estimated capacitances can be checked by comparing calculated results using the partial-capacitance method with exact solutions for simple cases which are known rigorously (such as two charged, parallel bare wires) or which can be solved to any desired degree of accuracy by summing multiple images.

In the regions where the grid is defined by concentric circles and radial lines, the partial capacitances in the radial direction must be just the capacitance between two concentric cylinders, with radii equal to the radii of the concentric circles of nodes, apportioned between the different nodes proportional to the angular spacing of the radial mesh lines. This choice is necessary so that this partial-capacitance method

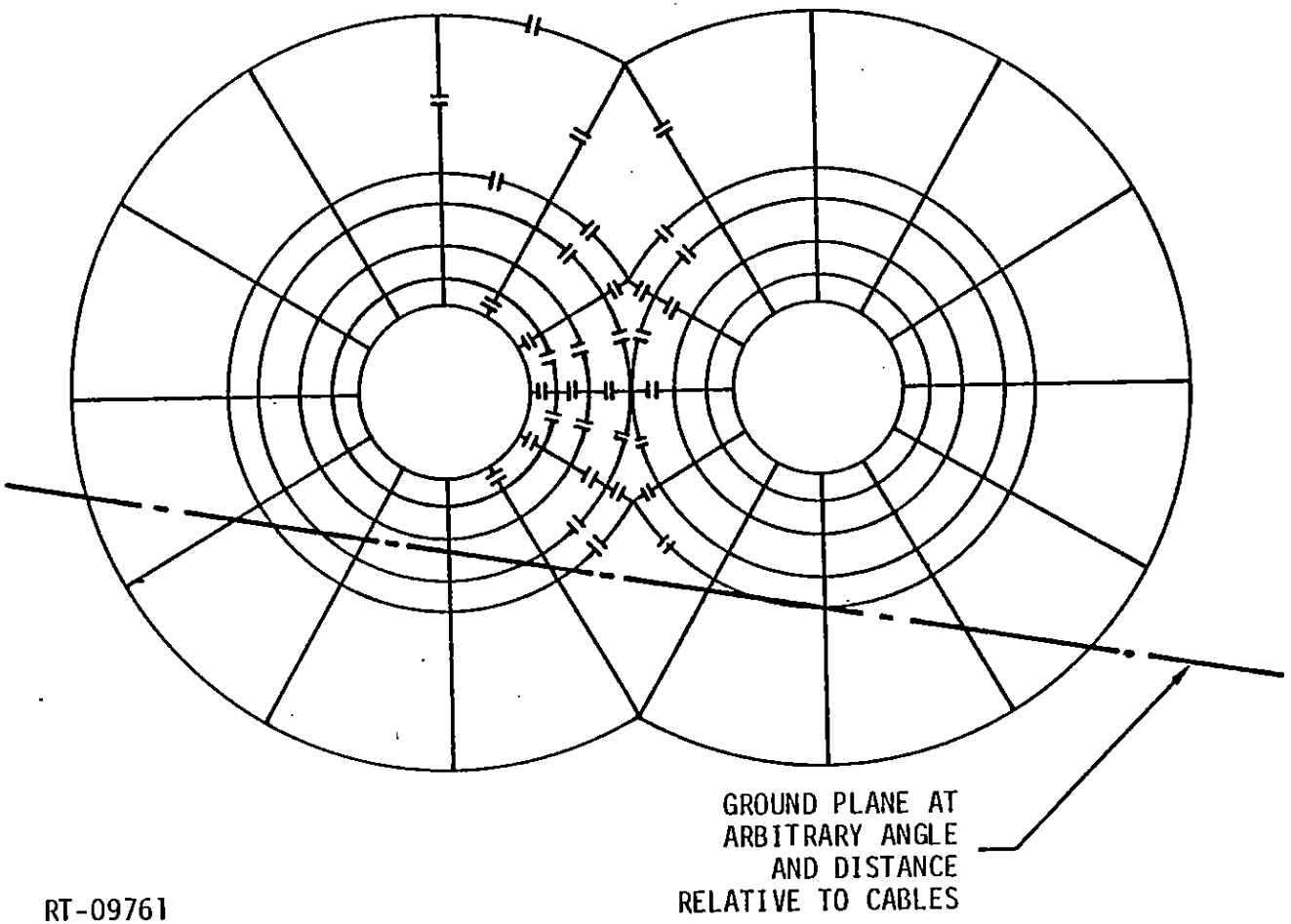

Figure A-1. Typical mesh grid for two parallel unshielded cables. (Each line between nodes is connected by a capacitor (||) as illustrated for a few lines; cable dielectric could coincide with any concentric circle that does not intersect the ground plane.)

will give the correct voltage difference for two concentric shells of charge at the radii of the nodes. Unfortunately, the choice of capacitances is not as clear in the azimuthal direction and in the intersection regions between wires and with the ground plane. For a very large rectangular grid, the correct capacitances are just the capacitances for a planar capacitor with an area and plate separation corresponding to the spacing of the rectangular grid. If the number of radial mesh lines in the cylindrical mesh is fairly large, each pie-shaped wedge will approximate a rectangular grid and the azimuthal capacitances can be estimated from the formula for a planar capacitor. Consequently, the procedure that has been used thus far to estimate all capacitances except the concentric radial ones uses average areas and average separation distances in the equation for planar capacitor. Since there is a certain amount of judgment involved in this method, these capacitances can justifiably be varied within reasonable limits to produce agreement with known exact results. Then, once a procedure has been selected for estimating these capacitances, it will be used for all subsequent calculations. Thus far, only a limited amount of checking has been done with exact solutions, as discussed below.

The circuit equations for the partial-capacitance method have been programmed and checked out for two parallel unshielded wires. The matrix of equations has been arranged in a manner to take advantage of their approximately diagonal nature. This arrangement greatly reduces the required computer storage and running time for a given number of nodes. For example, five problems were run for a typical mesh for a total charge of $3.20, a large part of which was initial setup charges. As a check on the assumed capacitances, the potential differences between two bare wires was calculated by the method of multiple images for a line charge at various positions on the line joining the centerlines of the two wires. This essentially exact solution is shown in Figure A-2, along with the corresponding results, using the partial-capacitance code. The results from the latter method are consistently about 5% higher than the correct result. Since the discrepancy is always in the same direction, better agreement could undoubtedly be obtained by modifying the method of choosing the capacitances. A calculation was also made using a different mesh

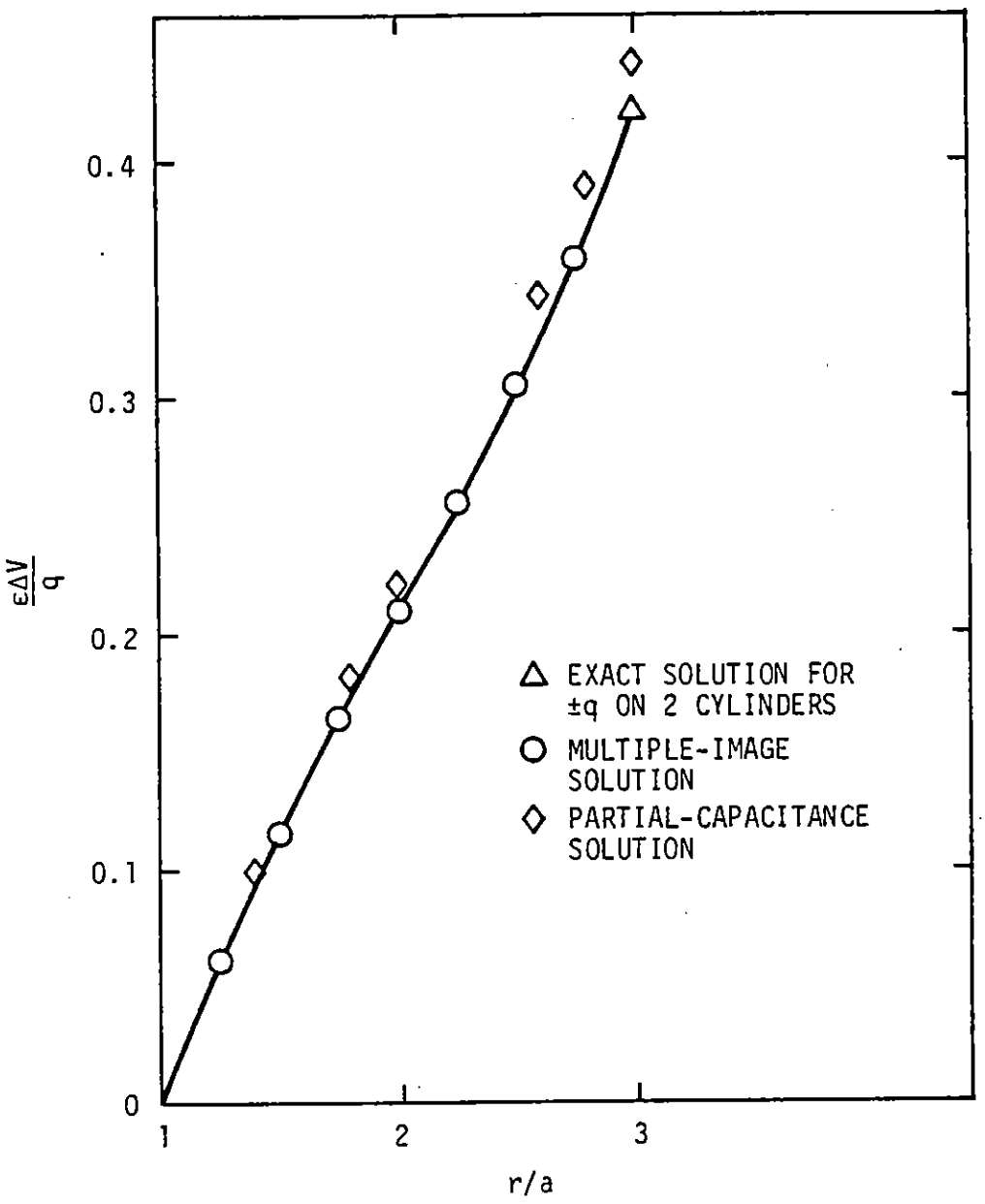

Figure A-2. Potential difference between two bare conducting cylinders with radii a, centerline-to-centerline separation = 4a, charge q on cylinder 1 and line charge (-q) at r from centerline of cylinder 1

distribution to check the sensitivity of the results. For the particular choices of mesh, the results were practically unchanged from the previous mesh results.

Although 5% accuracy is quite adequate for anticipated applications of this code, the comparison in Figure A-2 is not a sensitive test of all the capacitances. When the line charge is on the line between the cylinders, the potential differences between the cylinders is determined primarily by the radial capacitances on the line joining the cylinders. Since these radial capacitances must have certain values, as discussed previously, the good agreement in Figure A-2 is not surprising. On the other hand, when the line charge is not on the line between the cylinders, the capacitances in the azimuthal directions and at the intersections will have greater influence on the potentials. Therefore, for a more rigorous check on the estimated values for these capacitances, it is planned to make other comparisons between exact image solutions and the present code with the line charge at various node locations. This has not been done as yet.

4. PRESENT STATUS

The following is the present status of the codes for coaxial and unshielded cables.

4.1 COAXIAL CABLE

By the method described in Section 3.4, a simple, exact procedure is available for calculating the potential difference between a circular wire and its coaxial shield for any distribution of net charge in the dielectric and in the cable and its shield. Thus, all of the necessary elements are now available to perform the separate steps enumerated in Section 2 for the response of a coaxial cable to a pulse of radiation. The remaining task to obtain a working code for a coaxial cable is to combine these elements (described below) into one computer package.

1. Energy and Angular Distribution of Electrons Emitted from Walls of Container and Impinging on Cable

For a coaxial cable, practically all of the electrons emitted from the wall will be stopped in the sheath because their energies will be relatively low and they cannot penetrate the outer shield. From there, they will return via ground back to the emitting surface. If the shielding were perfect, this current would have no net effect on the response of a coaxial cable. For realistic cable terminations, this current could couple into the center wire and alter the cable signal. This coupling effect can be estimated separately from the bulk cable response, and it is not intended to include this effect in the cable code. However, since the charge from the cavity walls could be important for unshielded cables, this effect is described below for future reference in Section 4.2.

The densities, energies, and angular distributions of electrons which are emitted from the wall of the cavity and which impinge on the unshielded cables will be calculated by a computer code, called TEDIEM-PC, which was written by IRT under a different technical directive of this contract. For low-intensity pulses, the impinging flux is just the flux from an infinite irradiated plane which crosses an imaginary surface at the position of the cable. However, for high-intensity space-charge-limited conditions, the presence of the cable will modify the flux of electrons which escapes from the infinite wall and reaches the cable.

2. Photon Attenuation through Cables

The attenuation of the photon beam through the various materials of a cable could be calculated by standard photon transport routines. However, except for a few special cases, the photon attenuation is given reasonably well by a simple exponential decay, with an attenuation length that is a function of the photon wave length and the material that is being traversed. Thus, for any path through the cable materials, the incident spectrum will be modified, using exponential decays for various photon energies, as it passes through each layer of material.

3. Charge Transfer Across Metal-Dielectric Interfaces and in Bulk of Dielectric

There are various Monte Carlo codes, such as SANDYL, which calculate both the photon attenuation (see above) and the resulting charge transfer in the target materials. However, such codes require considerable computer running time to give acceptable statistical results. For most applications for which this cable code is intended, simpler approximate methods for estimating the charge transfer give adequate accuracy. One such method is the QUICKE2 code (Ref. 2). This code first calculates the "bulk" forward and backward currents of electrons due to the attenuated photon spectrum at the particular point in the bulk. It then calculates the number, energy, and angular distribution of electrons photo-emitted across an interface into vacuum, expressed in terms of the bulk currents.

Due to its relative simplicity, it is anticipated that the QUICKE2 code will be incorporated as a subroutine in our cable code to give the forward and backward charge transport information at the material interfaces and in the bulk of the dielectric. At each point in the material, the appropriate attenuated photon spectrum (see 2 above) will be used.

4. Charge Deposition

The potential difference between the conductors depends on the net charge on each conductor and the amount and distribution of trapped charge in the dielectrics.

For a coaxial cable, secondary electrons from the walls (item 1 above) do not affect the cable potential differences, so they can be ignored. Thus, the total charge distribution in a coaxial cable is due to the photon spectrum incident on the cable.

The net charge in a conductor will be just the net charges, calculated by QUICKE2, which are emitted from the conductor into the dielectric and from the dielectric into the conductor. This net charge will be found for both the cable and the sheath to provide a check on charge conservation.

The distribution of trapped charge in the dielectric depends on the energy, density, and angle of the emitted electrons and the ranges of the electrons as a function of energy in the dielectric. It is planned that tables of electron ranges versus energy for various common dielectric materials will be incorporated into the code and that a lookup procedure will be used to find the desired values. The distribution of trapped charge in the dielectric will be determined by applying these ranges to the emitted electron spectra from QUICKE2. Just how detailed this distribution information must be to provide adequate data for potential difference calculations has not been determined as yet. It may be that only the centroid of the charge distribution will be required, or perhaps an average exponential distribution can be assumed. These details are now being worked out.

For unshielded cables, essentially the same procedure will be used. However, in this case, the total density of charge emitted from the walls and captured by the cables must be found to give the deficit of charge in the ground plane (wall). The same range-energy tables described above will be used to determine the penetration of the electrons from the walls into the cable dielectrics.

5. Potential Differences and Current Generators

Using the charge distributions from item 4 for a coaxial cable, the charge at every radius in the dielectric will be averaged over the full azimuthal angle, as discussed in Section 3.4. The radial part of Poisson's equation in cylindrical coordinates will be integrated to obtain the potential difference ΔV between the cable and its shield. The corresponding current generator per unit length of the cable is

$$I = C\Delta V \frac{\dot{\gamma}}{\gamma} \quad ,$$

where C is the capacity between the cable and its shield per unit length of cable, $\dot{\gamma}$ is the instantaneous dose rate due to the pulse, and γ is the total dose which created ΔV.

6. Transmission-Line Code

When the effect of induced conductivity in the dielectric due to the instantaneous dose rate can be neglected, the transmission-line equations are quite straightforward. IRT has written a computer code which can accept a current generator driving function as a function of position and time and then calculate the response of the cable. If the induced conductivity is not negligible but is still only a function of time (for example, for normal incidence of the wave on the cable), the basic transmission-line code can be modified relatively simply to include the instantaneous conductance G in the basic LC circuits. However, the computer running time would be increased somewhat. Finally, when the conductance is a function of both position and time, the transmission-line equations would have to be modified even more and the computer running time would also increase. Initially, for the coaxial cable, it is planned to consider only the case of zero induced conductivity.

4.2 UNSHIELDED CABLES

The only significant differences in the code for unshielded and coaxial cables, except for obvious geometrical changes, are the trapping of secondary electrons from the cavity walls by the dielectric of the unshielded cable and the method for calculating the potential differences for the unshielded cables.

The electrons from the cavity wall that are trapped in the cable dielectric will add to the charge distribution which causes the potential difference. The compensating charge will remain in the wall (ground plane), as discussed in Section 4.1. The methods which will be used to calculate the characteristics of the electrons that are emitted from the cavity wall and reach the cable and the resulting distribution of trapped charge in the cable dielectric were discussed in items 1 and 4, respectively, of Section 4.1.

The code for calculating the potentials by the partial-capacitance method has been programmed for two wires, and the techniques for choosing the values of the capacitances are being evaluated. Once this evaluation

is completed and a standard procedure for selecting the capacitances is agreed upon, the code for the coaxial cable, described in Section 4.1, could be extended or modified to also handle two unshielded wires. The main changes will be the geometrical description of the cables so that the charge depositions can be properly specified relative to the partial-capacitance mesh.

APPENDIX B

POTENTIAL DIFFERENCE BETWEEN TWO CONDUCTING CYLINDERS DUE TO A LINE CHARGE BETWEEN THEM

As stated in Section 3.4, the potential difference between two conducting cylinders due to a line charge q between them is identically equal to the potential between the cylinders if the charge q were distributed uniformly in a thin cylindrical shell at the same radius as the line charge. This conclusion applies both when the volume between the cylinders is completely filled with a material with a uniform dielectric constant and when there are cylindrically symmetric gaps between the dielectric and the conductors.*

The above result is proved below for the case of a uniform dielectric by summing the first few terms of the infinite series of images which results from a line charge between two conducting cylinders. The same result can be obtained using a direct solution of Laplace's equation by the method of harmonics†, but for brevity, this proof is not presented here. This last method can also be used to obtain the desired result when the dielectric does not fill the space between the two cylinders and cylindrically symmetric gaps exist between the dielectric and the conductors.

Figure B-1 illustrates two concentric cylinders, with radii a and b, and a line charge q at radius r. For this proof, it is assumed that the compensating charge (-q) is all on the inner cylinder, but a similar proof can be obtained when (-q) is on the outer cylinder or distributed arbitrarily between the two cylinders.

The best way to apply the method of images for this problem is to first image the real charge q in the cylinder with the compensating charge

---

*A similar conclusion is valid for a point charge between two conducting spheres.

†W. K. H. Panofsky and M. Phillips, Addison-Wesley Publishing Co., Reading, Mass. (1955).

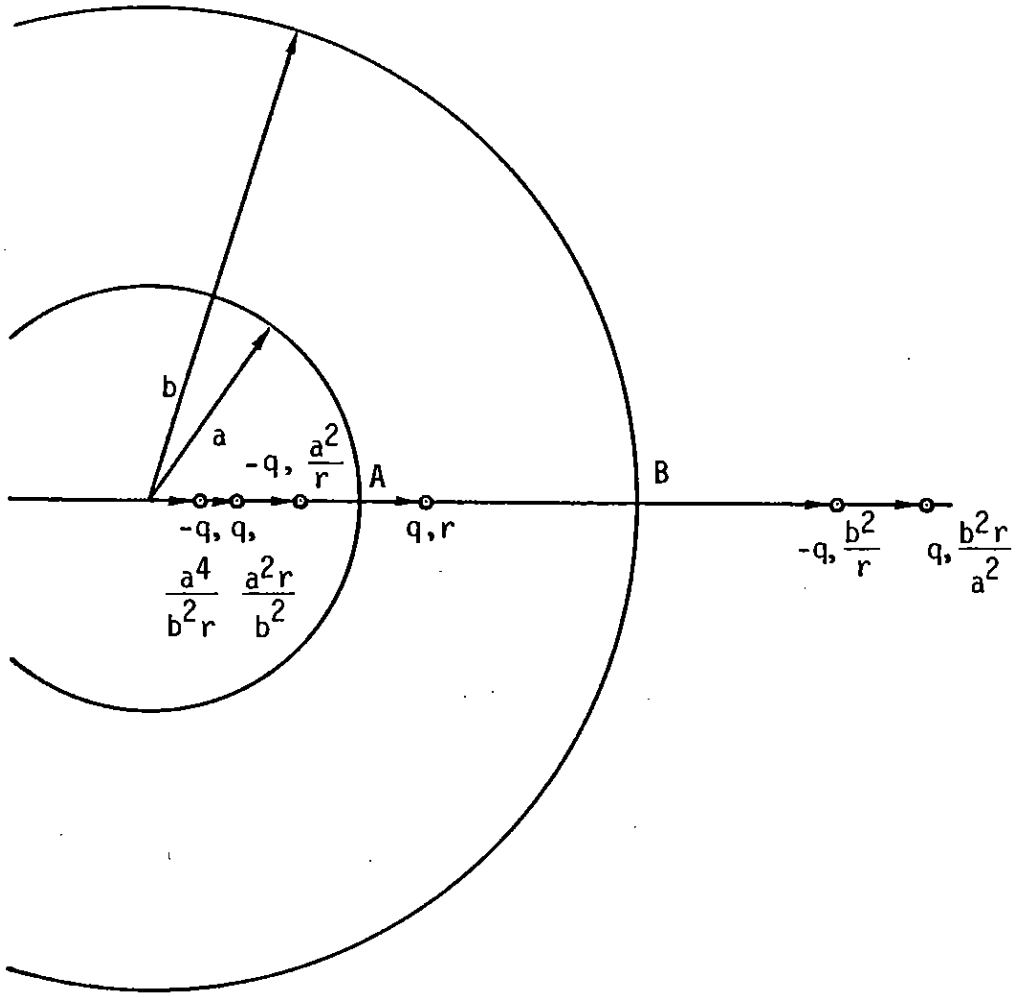

RT-09763

Figure B-1. First few images of infinite series for a line charge q between concentric conducting cylinders

(inner cylinder in this case) and thereafter image the neutral pair of line charges (±q) across the appropriate cylinders. By this method, the charge on each cylinder, as determined by summing all the images inside the inner cylinder and outside the outer cylinder, will always be correct and the series can be terminated at any time without violating conservation of charge.

The first few images are shown in Figure B-1 and are summarized below with their radii from the centerline of the cylinders. Note that the image of q at radius x in a cylinder of radius y is a charge -q at radius $\frac{y^2}{x}$.

1. Real q at r
2. Image of (1) in inner cylinder

   -q at a^2/r
3. Images of (1) and (2) in outer cylinder

   -q at $\frac{b^2}{r}$

   +q at $\frac{b^2 r}{a^2}$
4. Images of (3) in inner cylinder

   +q at $\frac{a^2 r}{b^2}$

   -q at $\frac{a^4}{b^2 r}$
5. Images of (4) in outer cylinder

   -q at $\frac{b^4}{a^2 r}$

   +q at $\frac{b^4 r}{a^4}$

The potential difference between the two cylinders, calculated for convenience between points A and B in Figure B-1, is given below with the contribution from each pair of line charges kept separate.

$$\Delta V = V_B - V_A = \frac{q}{2\pi K\varepsilon_o} \ln \left[\left(\frac{r-a}{b-r} \right) \left(\frac{b - \frac{a^2}{r}}{a - \frac{a^2}{r}} \right) \right. \qquad \text{due to (1) and (2)}$$

$$\cdot \left(\frac{\frac{b^2 r}{a^2} - a}{\frac{b^2 r}{a^2} - b} \right) \left(\frac{\frac{b^2}{r} - b}{\frac{b^2}{r} - a} \right) \qquad \text{due to (3)}$$

$$\cdot \left(\frac{a - a^2 r/b^2}{b - a^2 r/b^2} \right) \left(\frac{b - a^4/b^2 r}{b - a^4/b^2 r} \right) \qquad \text{due to (4)}$$

$$\cdot \left(\frac{\frac{b^4 r}{a^4} - a}{\frac{b^4 r}{a^4} - b} \right) \left(\frac{\frac{b^4}{a^2 r} - b}{\frac{b^4}{a^2 r} - a} \right) \qquad \text{due (5)}$$

$$\left. \text{etc.} \right] \; .$$

In this equation, K is the dielectric constant of the insulator which is assumed to fill the region between the cylinders.

This equation can be written in a more revealing form as follows.

$$\Delta V = \frac{q}{2\pi K\varepsilon_o} \ln \left[\frac{r}{a} \cdot \left(\frac{b - \frac{a^2}{r}}{b - r} \right) \right. \qquad \text{due to (1) and (2)}$$

$$\cdot \left(\frac{b - r}{b - \frac{a^2}{r}} \right) \left(\frac{b^2 - a^3/r}{b^2 - ar} \right) \qquad \text{due to (3)}$$

$$\cdot \left(\frac{b^2 - ar}{b^2 - a^3/r}\right)\left(\frac{b^3 - a^4/r}{b^3 - a^2 r}\right) \quad \text{due to (4)}$$

$$\cdot \left(\frac{b^3 - a^2 r}{b^3 - a^4/r}\right)\left(\frac{b^4 - a^5/r}{b^4 - a^3 r}\right) \quad \text{due to (5)}$$

$$(\text{etc.})\Big] \quad .$$

The series can be terminated when the remaining terms contribute negligibly to ΔV. It will be noted that the terms in the second bracket for one set of images exactly cancels the terms in the first bracket for the next set of images. Therefore, after n sets of images, the equation for ΔV is just

$$\Delta V = \frac{q}{2\pi K\epsilon_o} \quad \ell n\left[\left(\frac{r}{a}\right)\left(\frac{b^{n-1} - a^n/r}{b^{n-1} - a^{n-2} r}\right)\right] \quad .$$

Since a is less than r and r is less than b, one can always make n large enough so that the terms involving a are negligible compared to b^{n-1}. In that case,

$$V = \frac{q}{2\pi K\epsilon_o} \quad \ell n\left(\frac{r}{a}\right) \quad ,$$

which is just the potential for charge -q on a cylinder of radius a and a cylindrical shell of charge q with radius r. Since there is no electric field outside the shell of charge at radius r, this formula is also the potential between the inner cylinder and any point outside the radius r — in particular, the potential between the two conducting cylinders.

APPENDIX C

CABLE CODE TEST PROBLEM FOR COMPARISON WITH THE MISSION RESEARCH CORPORATION BCABLE CODE

Because two EMP cable pick-up codes were to be used in this joint effort, it was felt that a test problem should be run to ensure that both codes gave similar results for the same excitation. A test problem was defined as described in the following paragraphs, and both the MRC BCABLE code and the IRT CABLE code were exercised and compared.

The IRT frequency-domain multiconductor transmission-line code CABLE was used to determine the EMP-induced currents on the three-conductor line above ground plane, as sketched in Figure C-1a. The exciting field is an incident double exponential EMP given by

$$\exp(t) = 5.2 \times 10^4 \left[\exp(-4 \times 10^6 t) - \exp(-4.76 \times 10^8 t)\right] \text{ V/m} . \quad (1)$$

This field is assumed to be tangentially incident with vertical polarization. Doubling of the vertical field due to reflection yields a peak vertical field of ∿100 kV/m. The loading of this multiconductor line is shown in Figure B-1b. Note that the 1F series capacitors are nominally a short circuit for the frequencies of interest.

The frequency-domain analysis was performed at 256 frequencies (up to 100 MHz), with the corresponding time-domain results obtained by use of a FFT algorithm. The results given in Figures C-2 through C-9 consist of time-domain individual wire and bulk current for both ends of the cable.

This problem was run on GA's UNIVAC 1108 computer and required ∿25 seconds of CPU time for execution.

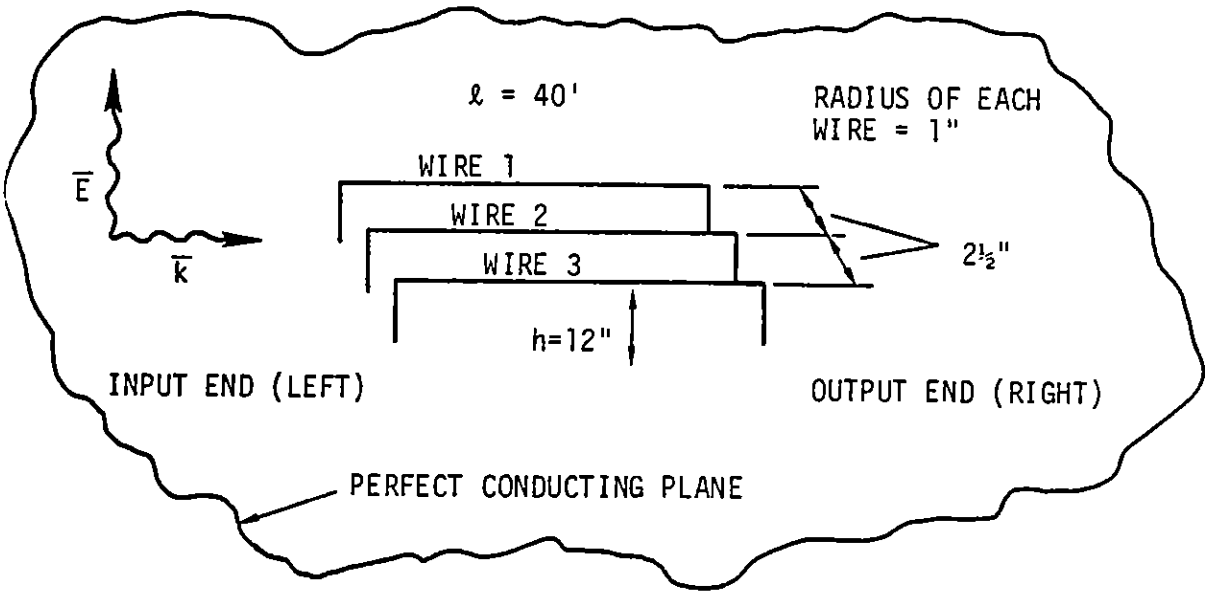

Figure C-1a. Cable geometry (not to scale)

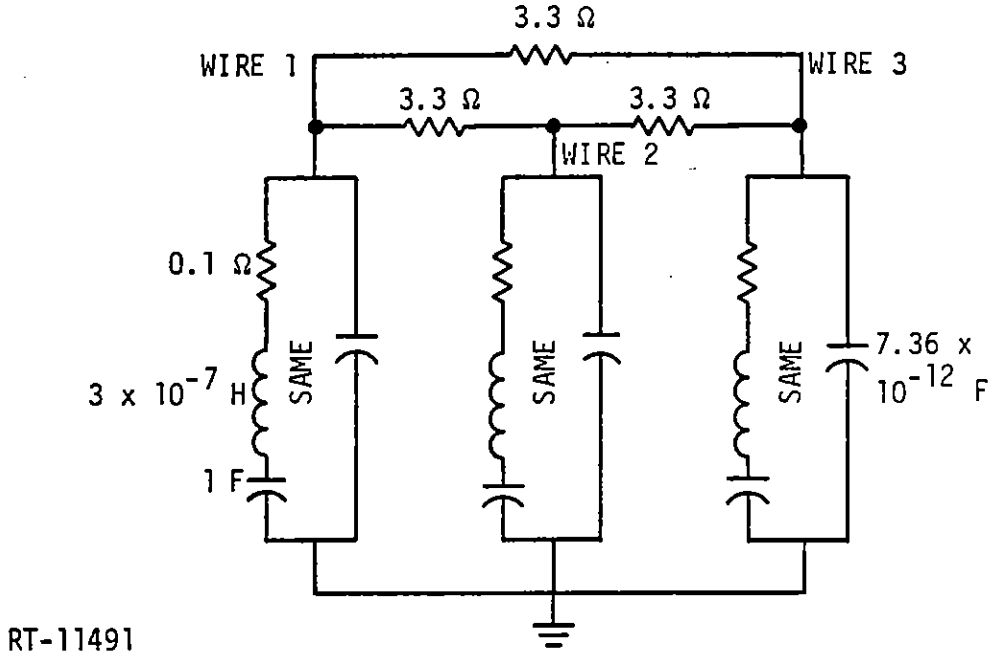

Figure C-1b. Cable loading; same at both input and output ends

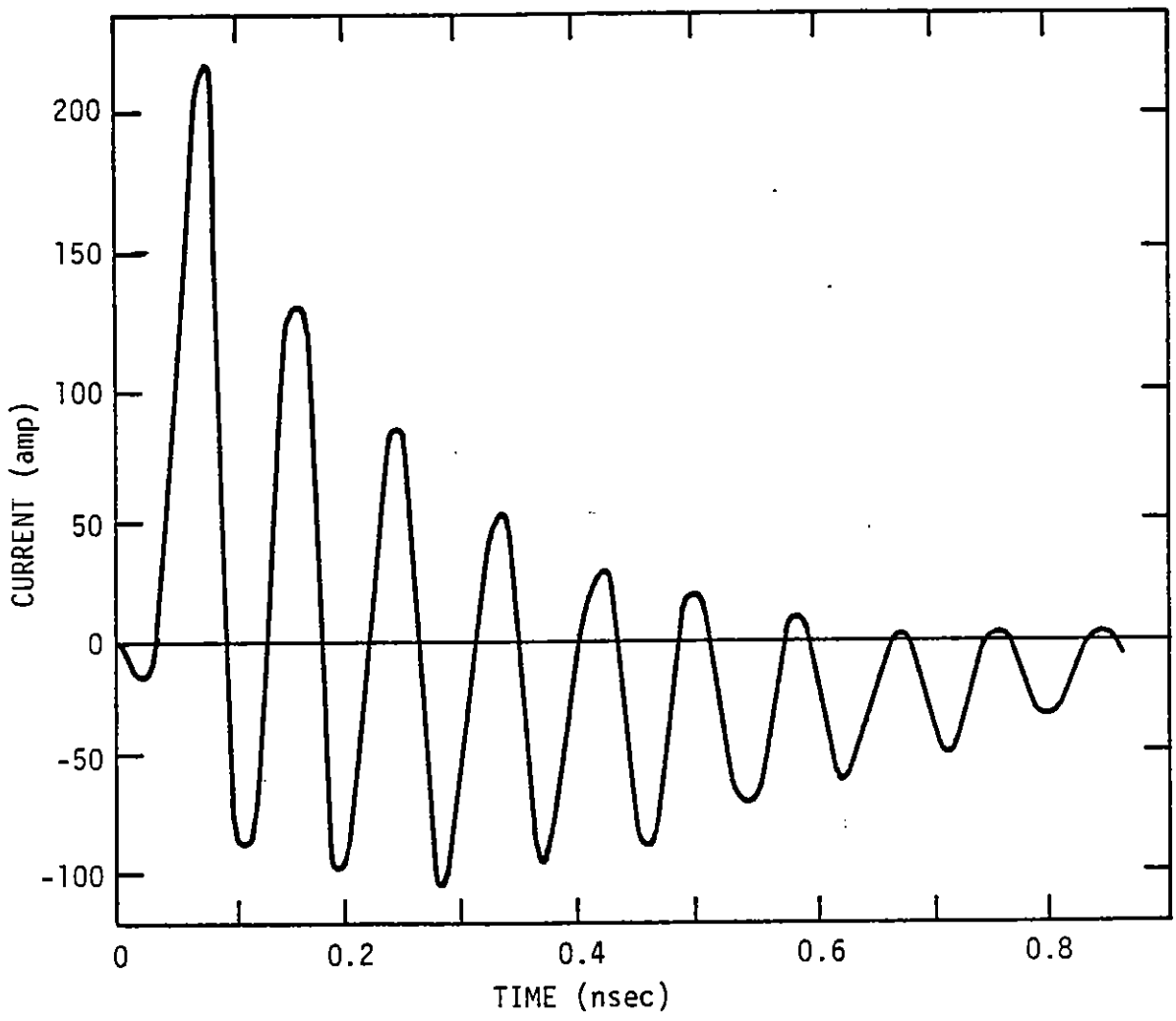

Figure C-2. Current on left end of wire 1

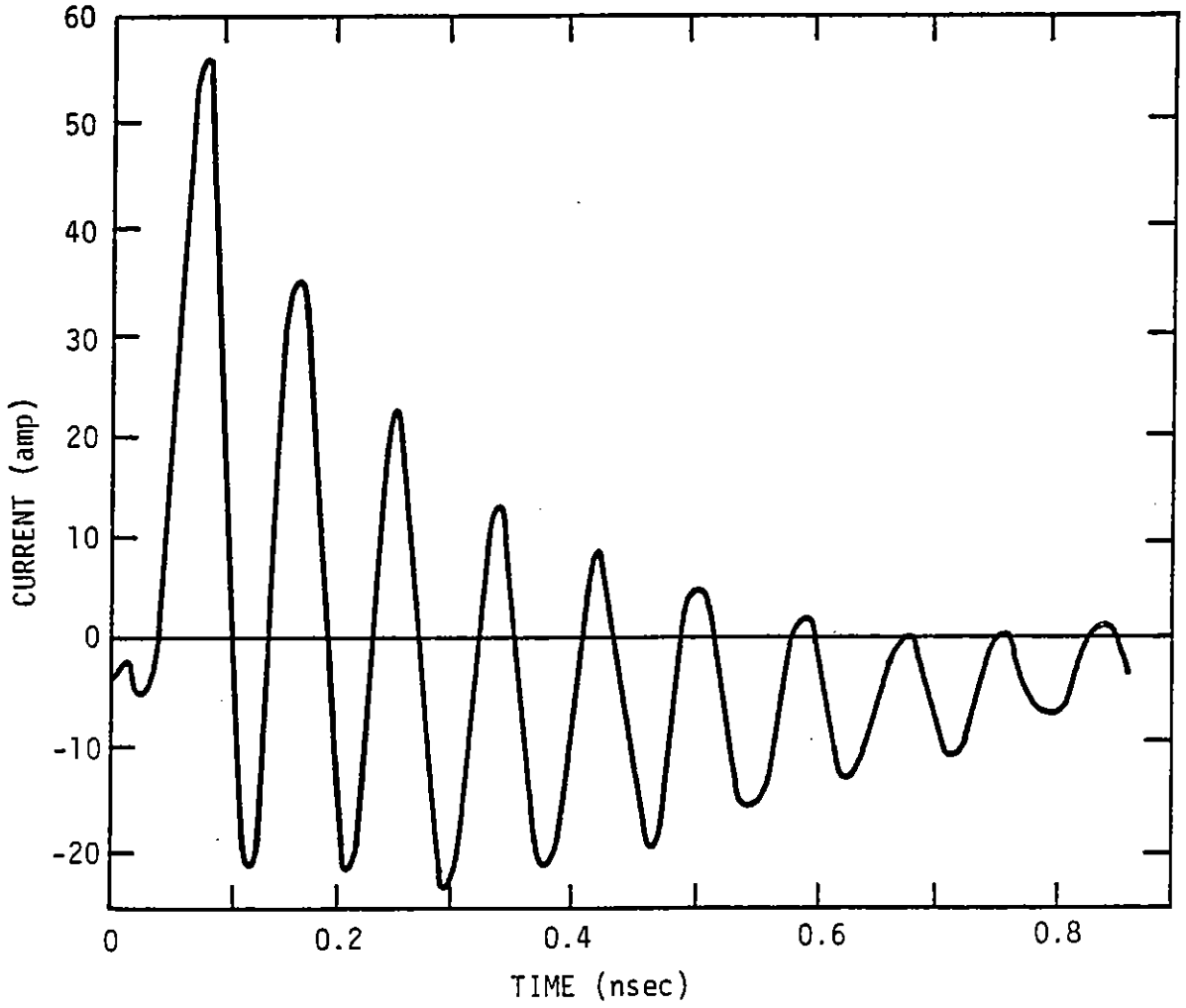

Figure C-3. Current on left end of wire 2

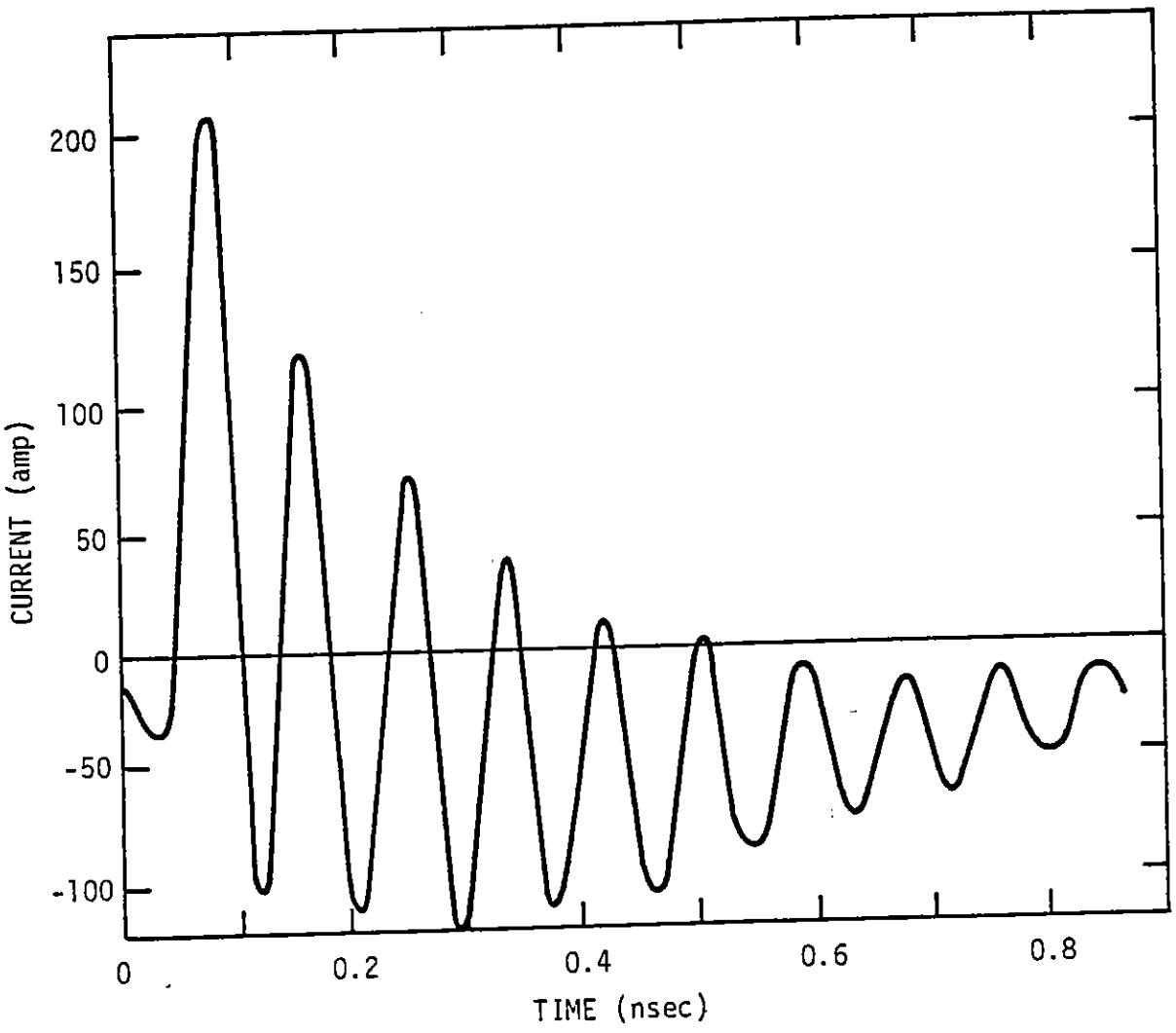

Figure C-4. Current on left end of wire 3

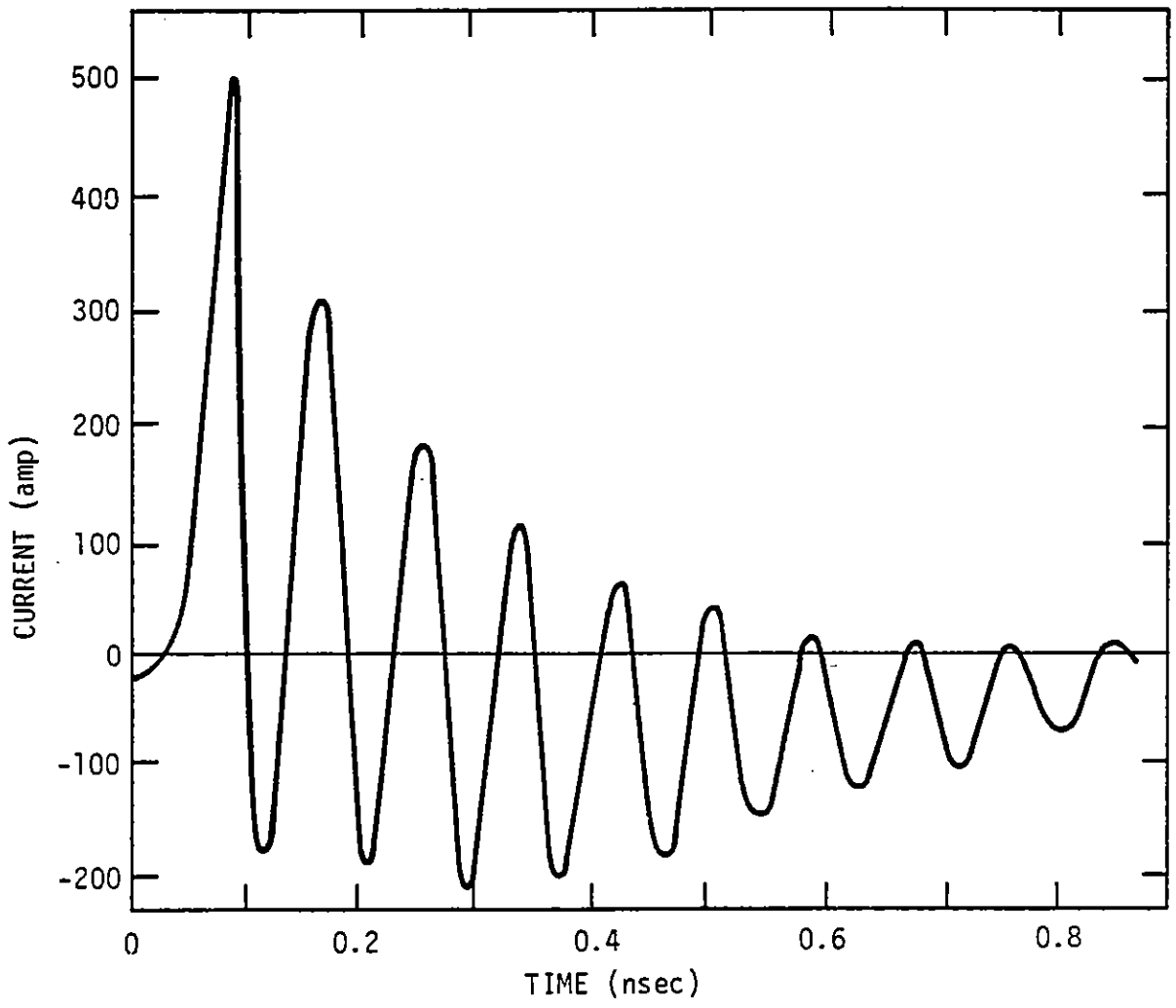

Figure C-5. Bulk current, left end

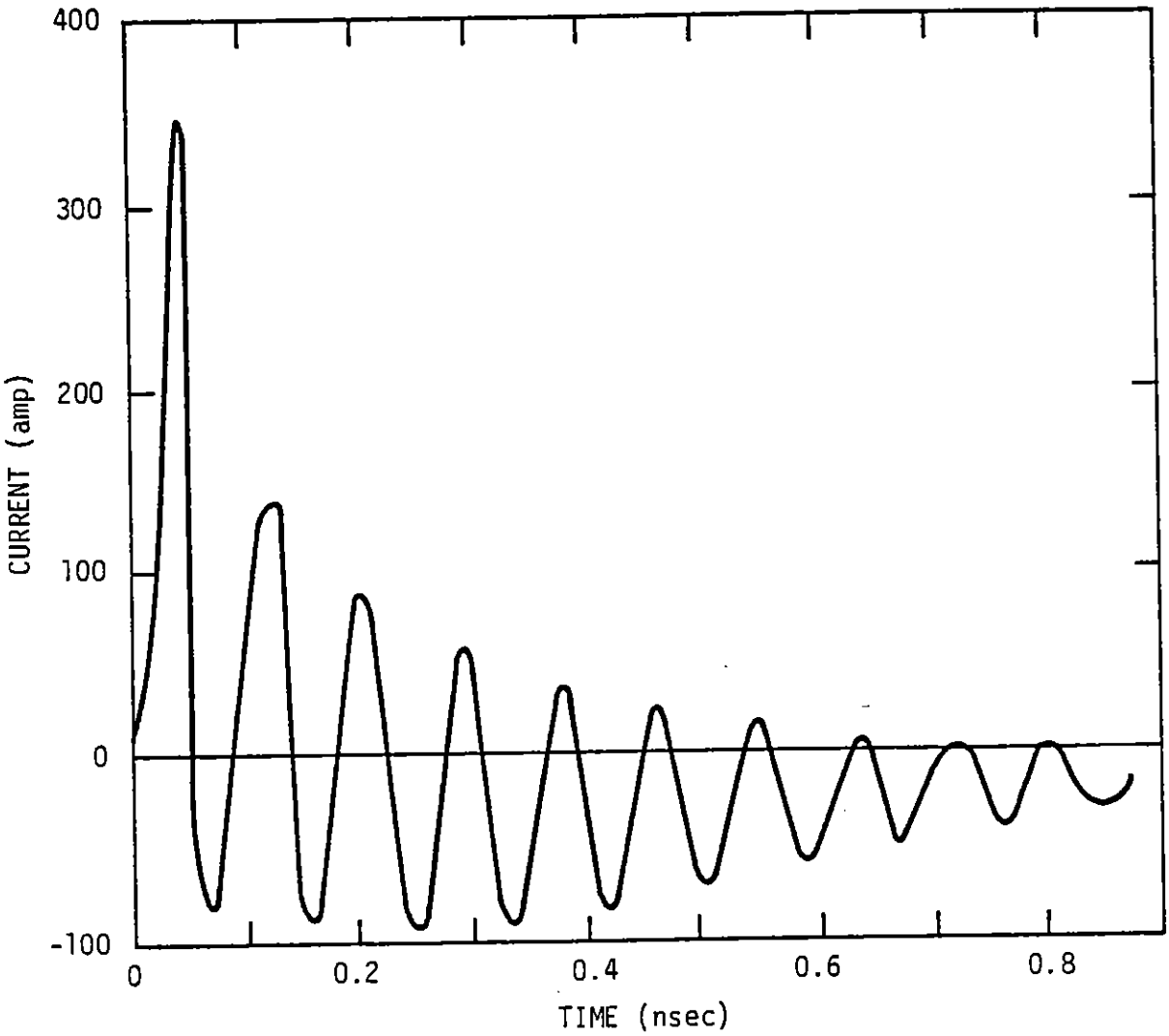

Figure C-6. Current at right end of wire 1

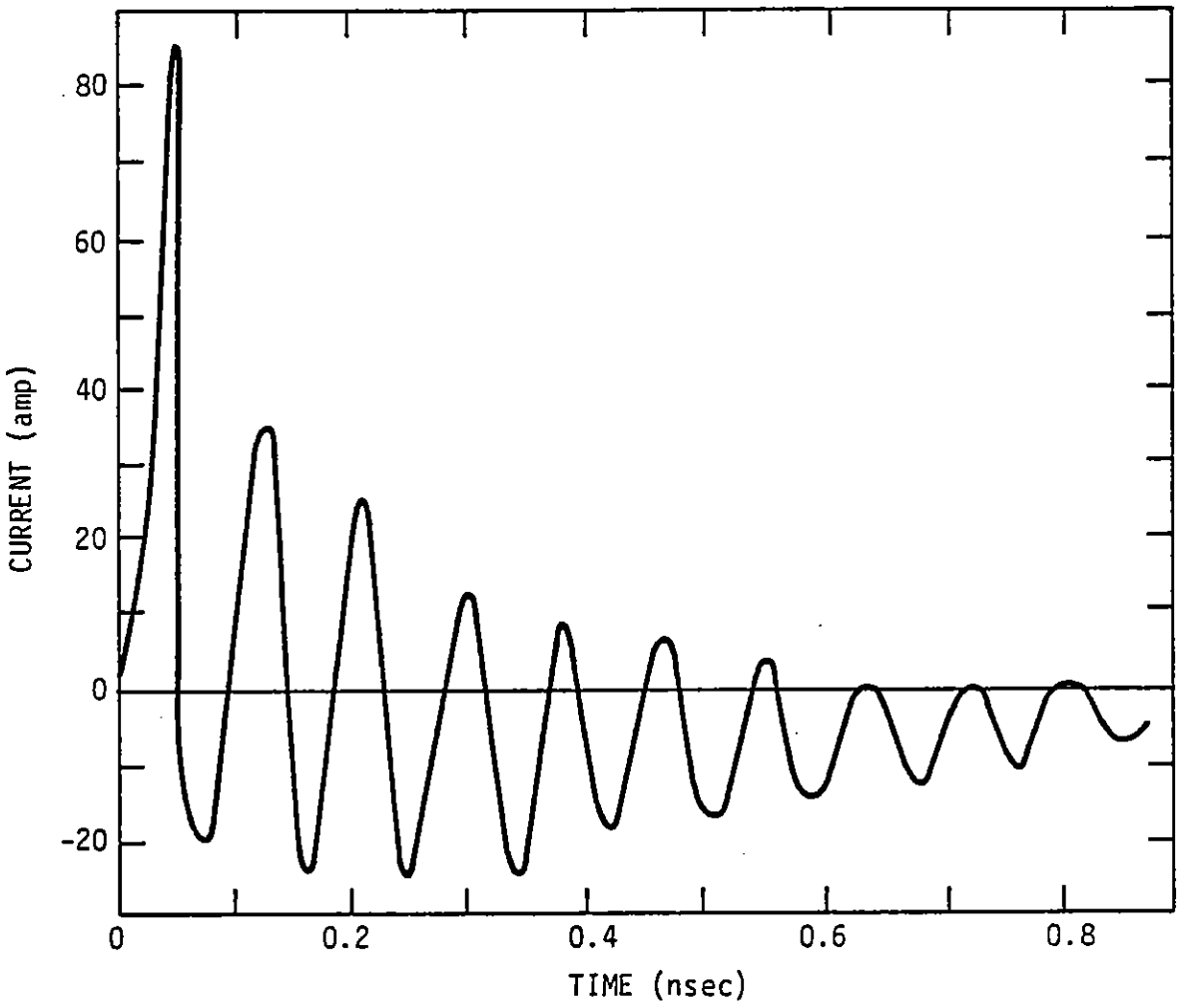

Figure C-7. Current at right end of wire 2

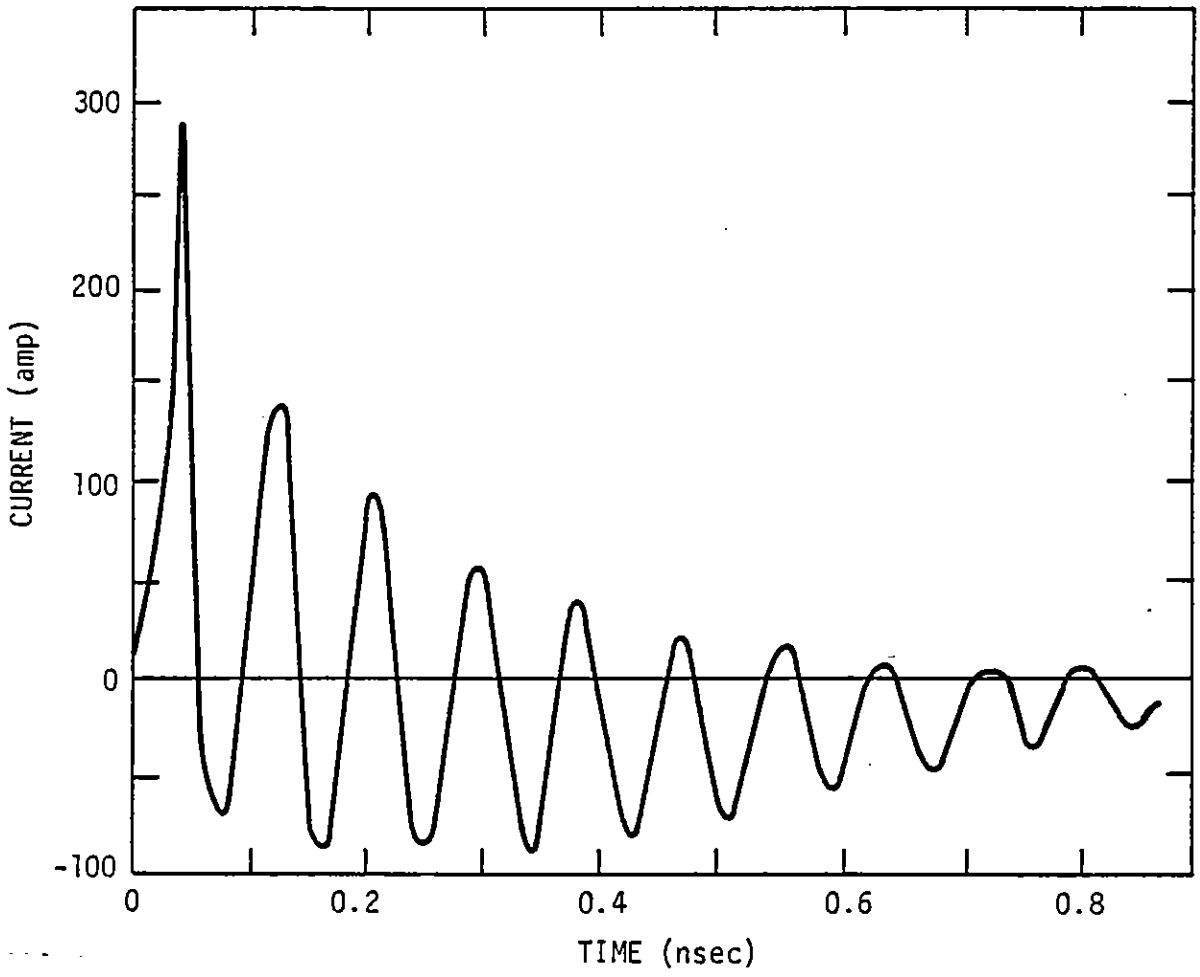

Figure C-8. Current at right end of wire 3

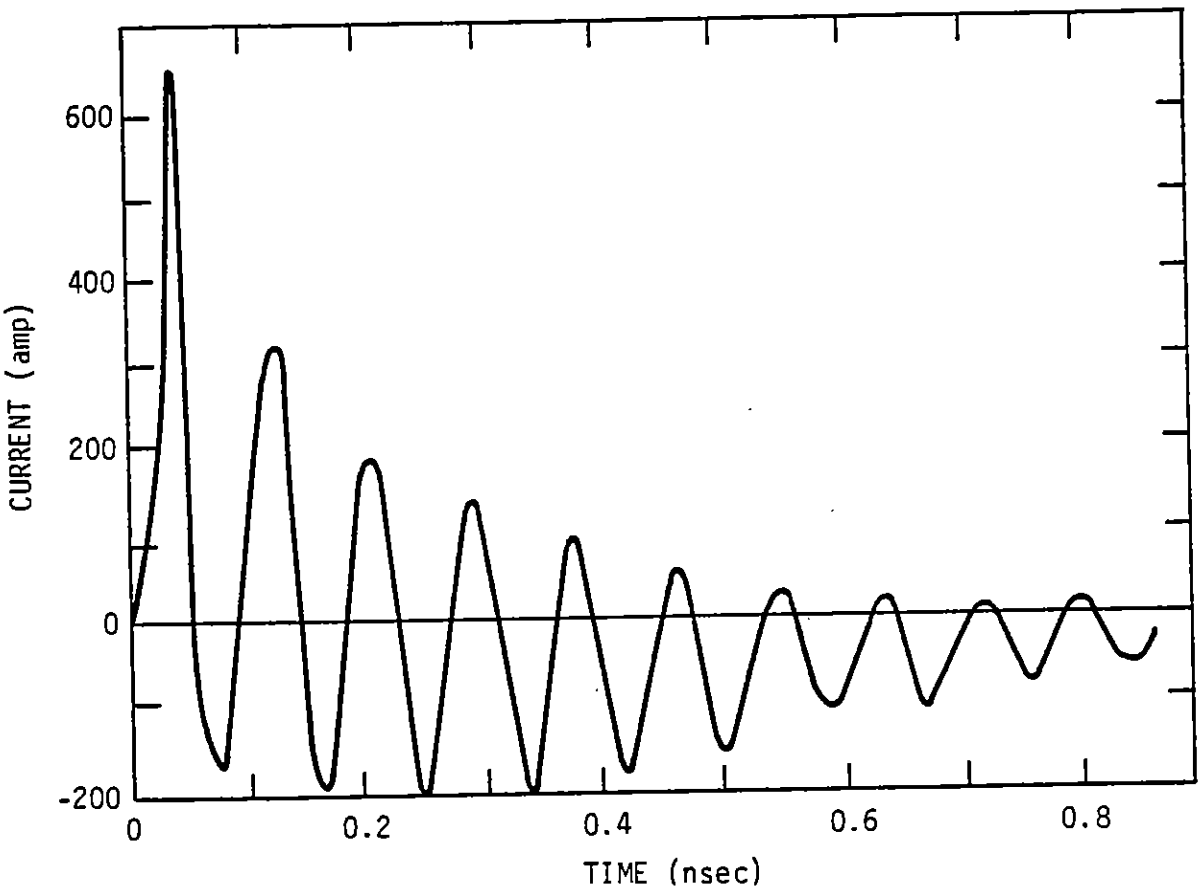

Figure C-9. Bulk current, right end

The same problem was run by MRC using the BCABLE code. Results of the MRC calculation are shown in Figures 15 through 20 of Part 2 for each of the individual wire currents. It is evident that the two results do not agree well. The MRC results have numerous "spikes," while the IRT results appear to be smoothly damped sinusoidal currents. The peak amplitude of the two results do not compare favorably either.

It is difficult to say which solution is correct, if either. However, we do note that the cable configuration and excitation polarization and orientation are such that the response on wires 1 and 3 must be identical due to symmetry considerations.

The bottom line of this comparison is that differences in results and conclusions obtained from the two codes, if any, may be a result of problems in the codes rather than differences in modeling excitation source terms.

REFERENCES

1. A. J. Woods et al., "SKYNET Program Quarterly Report," IRT document INTEL-RT 8121-019, April 25, 1975.
2. R. Stettner, "A Description of the SEMP Code," Mission Research Corp. report to be published August 1975.
3. T. A. Tumolillo et al., "SKYNET Program Current-Injection Predictions," Vols. 1, 2, and 3, IRT report INTEL-RT 8121-007.
4. W. L. Chadsey and D. Edelman, "Internal Electromagnetic Pulse: An Investigation of Cable Response to the IEMP Environment," HDL-0086, June 1972.
5. J. P. Woodruff and D. C. Oakley, "Computer Simulation of IEMP Cable Response (U)," IEMP Symposium, February 1973, DASIAC SR-146, p. 6-3 (Secret-Restricted Data).
6. H. W. Kruger, "Design Considerations for IEMP-Insensitive Transmission Lines (U)," IEMP Symposium, February 1973, DASIAC SR-146, p. 10-1 (Secret-Restricted Data).
7. R. L. Fitzwilson et al., "Radiation-Induced Currents in Shielded Multi-Conductor and Semi-Rigid Cables," IEEE Trans. Nucl. Sci. NS-21 (1974).
8. T. M. Flanagan et al., "Investigation of Cable Response to X-Radiation (U)," AFWL-TR-73-295, 30 May 1973 (Secret-Restricted Data).
9. R. E. Leadon, M. Wilson, and R. Trybus, "Cable Response Solution Techniques for SGEMP," Supplement I, IRT report 8111-078, May 1975.
10. "System-Generated Electromagnetic Pulse (U)," TRW report 16439-57-013-601, September 5, 1973 (Secret).
11. E. F. Vance, "Shielding Effectiveness of Braided-Wire Shields," IEEE Trans. EMC, EMC-17, No. 2, May 1975.
12. K. S. H. Lee, "Balanced Transmission Lines in External Fields," AFWL EMP Interaction Note 115, July 1972.
13. E. P. dePlomb, and A. J. Woods, "TEDIEM-RZ and -RΘ: Two-Dimensional, Time-Dependent Computer Codes," IRT report RT-A12525, March 1973.
14. E. P. Wenaas, "Lumped-Element Modeling of Satellite SGEMP Excitation," IEEE Trans. Nucl. Sci. NS-21, December 1974.
15. A. J. Woods and T. N. Delmer, "Rod over Ground Plane Code, TEDIEM-PC," AFWL-TR-74-313, November 1974.
16. K. S. H. Lee, "Cable Response to System-Generated EMP," AFWL EMP Theoretical Note 176, April 1973.
17. R. Plonsey and R. E. Collin, Electromagnetic Fields, McGraw-Hill (1961), pp. 96-101.